BILINGUAL PUBLISHING GROUP

**Research in Ecology**
https://journals.bilpubgroup.com/index.php/re

**ARTICLE**

# Variation Patterns of Plant Root and Leaf Functional Traits, and Ecosystem Functioning: Research Progress and Prospect

***Hailing Liao*** [1,2*] **, *Mohd Nazre*** [1] **, *Beilei Yin*** [1,3] **, *Johar Mohamed*** [1]

[1] *Department of Forest Science and Biodiversity, Faculty of Forestry and Environment, Universiti Putra Malaysia, Serdang 43400, Malaysia*

[2] *Nanchang Junhan Environmental Protection Consulting Co., Ltd., Nanchang 330224, China*

[3] *College of Forestry Engineering, Guangxi Eco-engineering Vocational and Technical College, Liuzhou 545003, China*

## ABSTRACT

Plant root and leaf functional traits link individual adaptation to ecosystem functioning, yet their coordination mechanisms remain insufficiently understood. We established 18 plots along an elevational gradient (1200–2700 m) in the Qinling Mountains, measuring 12 key traits of 12 tree species and assessing three ecosystem functions. Results showed: (1) Traits exhibited significant interspecific variation with environmental gradients explaining 42–58% of variance; (2) Root-leaf coordination was moderate globally (r = 0.58 for specific leaf area and specific root length) but strengthened significantly under high-elevation stress (r increased from 0.38 to 0.72), supporting the environmental stress hypothesis; (3) Principal component analysis identified three ecological strategies—competitive, stress-tolerant, and intermediate types—cumulatively explaining 78.6% of total trait variance, with environmental factors predicting strategy classification at 82.3% accuracy; (4) Structural equation modeling revealed environmental effects were predominantly transmitted through root traits (β = 0.62) to leaf traits (β = 0.43), with 61.3% of effects mediated by traits rather than direct pathways; (5) Specific leaf area and leaf nitrogen jointly explained 61.2% of productivity variation, while litter nitrogen content controlled decomposition rates (r = 0.78), and the lignin:nitrogen ratio explained 65.6%

*CORRESPONDING AUTHOR:
Hailing Liao, Department of Forest Science and Biodiversity, Faculty of Forestry and Environment, Universiti Putra Malaysia, Serdang 43400, Malaysia; Nanchang Junhan Environmental Protection Consulting Co., Ltd., Nanchang 330224, China; Email: lhailling@126.com

ARTICLE INFO
Received: 6 November 2025 | Revised: 25 December 2025 | Accepted: 12 January 2026 | Published Online: 20 April 2026
DOI: https://doi.org/10.30564/re.v8i2.12690

CITATION
Liao, H., Nazre, M., Yin, B., et al., 2026. Variation Patterns of Plant Root and Leaf Functional Traits, and Ecosystem Functioning: Research Progress and Prospect. Research in Ecology. 8(2): 298–324. DOI: https://doi.org/10.30564/re.v8i2.12690

of decomposition variance. This research confirms functional traits as effective predictors of ecosystem functioning, providing theoretical foundations for trait-based ecosystem management under global change scenarios.

***Keywords:*** Plant Functional Traits; Root-Leaf Coordination; Trait Trade-Offs; Ecosystem Functioning; Elevational Gradient

# 1. Introduction

Plant functional traits, serving as a critical bridge connecting individual physiological processes to ecosystem functioning, have become a core paradigm in modern ecological research. Functional traits are defined as a set of measurable characteristics that significantly influence plant development, survival, growth, and mortality [1]. These traits, whether considered individually or in combination, provide important insights into understanding how ecosystems respond to environmental change and exert strong influences on ecosystem processes [2]. Plant traits represent the objective expression of plant adaptation to external environments, and ecosystem functional characteristics are reflected through the presence, absence, or abundance of specific plant traits [3]. Leaves, as the primary organs for photosynthesis and material production, constitute the key interface for water and gas exchange between plants and the atmosphere [4]. Leaf functional traits such as specific leaf area, leaf nitrogen content, and leaf dry matter content influence plant photosynthesis, water use efficiency, and nutrient uptake capacity [5]. The fine root system, including the hyphal network frequently colonized by mycorrhizae, is critical for plant water and nutrient acquisition [6]. Root functional traits such as root biomass, root length density, and root nutrient content influence plant nutrient uptake and soil resource utilization, playing a crucial role in material cycling and energy flow in forest ecosystems [7]. The capacity of plants to acquire resources and regulate water and nutrient uptake is determined by the functional traits of their roots and leaves. Therefore, a thorough understanding of the variation patterns and interrelationships of root-leaf functional traits is essential for predicting plant community dynamics and ecosystem processes [8]. However, current research exhibits significant knowledge gaps in the coordination mechanisms between aboveground and belowground functional traits, the regulatory roles of environmental factors, and how trait variation influences carbon and nitrogen cycling at the ecosystem level. These gaps urgently require a deepened understanding through comparative studies across multiple environmental gradients and multi-scale integrative analyses.

Research on root functional traits has revealed the diversity of plant belowground resource acquisition strategies and their ecological adaptive significance. Roots, as the key organs for plant-soil contact, have morphological and structural characteristics that directly reflect primary physiological functions. Root diameter plays a critical role in regulating root length, root-soil contact area, and mycorrhizal colonization rates, thereby influencing plants' capacity to acquire soil water and nutrients [9]. Plant root systems possess multi-order branching architectures, with different root orders exhibiting significant morphological and functional differences [10]. Among these, absorptive fine roots are the primary organs for plant water and nutrient resource acquisition [11]. Interspecific and intraspecific variation in root functional traits provides the foundation for understanding species coexistence and ecological strategies. Under different environmental conditions, greater variation in root traits among coexisting species within the same community can lead to diverse or complementary resource acquisition strategies, thereby reducing competition and promoting species coexistence [12]. Plants adapt to environmental changes through intraspecific variation in root functional traits, a phenomenon also termed root plasticity, which determines a species' capacity to adapt to varying resource availability and plays a key role in determining their ecological adaptability and geographic distribution patterns [13]. Studies have demonstrated that the magnitude of variation in fine root mean diameter across different climate zones follows the pattern: temperate < subtropical < tropical [14]. Fine root nitrogen content increases with root order, and the increase in angiosperms is approximately twice that of gymnosperms [15]. Research along latitudinal gradients has found that fine root biomass of European beech declines with increasing latitude,

potentially due to reduced soil water availability, while drought resistance of Scots pine increases with latitude, possibly due to selection pressure for drought tolerance in more arid environments [16].

The leaf economics spectrum theory provides a unified theoretical framework for understanding plant resource use strategies, revealing universal patterns of coordinated variation in plant leaf traits at the global scale. Specific leaf area, as a key parameter in plant ecology research, is defined as the one-sided area of a fresh leaf divided by its dry weight. It is an easily measurable indicator that correlates well with many plant traits such as relative growth rate, leaf gas exchange, photosynthesis, leaf lifespan, and leaf nitrogen content [17]. The global leaf economics spectrum proposed by Wright et al. [5] demonstrated that significant coordinated variation exists among physiological indicators, including specific leaf area, leaf nitrogen content, and photosynthetic rate. These traits form a continuous trade-off spectrum ranging from the "low investment-quick return" end (high specific leaf area, high nutrient content, rapid growth) to the "high investment-slow return" end (low specific leaf area, low nutrient content, slow growth, long leaf lifespan), reflecting evolutionary trade-offs among photosynthetic rate, structural costs, and leaf lifespan in vascular plants. This theory has been validated across multiple specialized habitats globally, including alpine plants on the Qinghai-Tibet Plateau, subarctic plants, and analyses of 46,085 vascular plant species worldwide. These studies and findings provide robust evidence for the regularity, stability, and universality of the leaf economics spectrum [18]. Leaf functional traits such as specific leaf area and leaf nitrogen content exhibit significant variation along latitudinal gradients. Plants in low-latitude regions often display higher specific leaf area and leaf nitrogen content, a pattern believed to be driven by higher temperatures and precipitation in low-latitude regions, promoting more rapid growth and photosynthesis.

The intrinsic linkages and trade-off relationships between aboveground and belowground functional traits are key to understanding plant holistic adaptive strategies, yet this research domain still exhibits numerous controversies and knowledge gaps. The intrinsic linkages and trade-off relationships between aboveground and belowground functional traits are key to understanding plant holistic adaptive strategies, yet this research domain exhibits critical controversies and knowledge gaps. These unresolved issues necessitate multi-gradient comparative studies to disentangle environmental, phylogenetic, and mycorrhizal effects on trait coordination mechanisms. Roots play a critical role in connecting aboveground and belowground processes. For specific ecosystem types, the morphology, architecture, and distribution of dominant plant roots influence, to a certain extent, the ecosystem's carbon processes, water balance, and biogeochemical cycling of mineral elements. Studying the linkages between plant roots and leaves is crucial for understanding how plant traits interact and how resources are used and allocated during plant growth, as ecosystem responses to global change depend on strong coupling between aboveground and belowground processes [19]. Experimental evidence has demonstrated that in herbaceous plants, fast-growing plants compared to slow-growing plants exhibit high leaf area and low tissue density corresponding to lower root tissue density, indicating coordinated variation between aboveground and belowground traits. Studies have found that leaf nitrogen content and tissue density are highly correlated with roots, suggesting that some root functional traits can be predicted by measuring readily accessible leaf functional traits. However, different studies have reached divergent conclusions regarding root-leaf trait relationships. Research on 55 herbaceous species in Inner Mongolian grasslands found that root-leaf trait relationships depend primarily on research scale and root order selection. Interspecific variation in specific root length increases with root order while intraspecific variation decreases, and the relationship with specific leaf area shifts from significantly positive to negative [20]. Studies of different geographic populations of coffee trees found no significant correlations between seven root traits and four corresponding leaf traits, and research on 13 European temperate tree species also concluded that the leaf economics spectrum cannot fully reflect the root spectrum. These contradictory research findings suggest that aboveground-belowground trait relationships may be modulated by environmental conditions, species types, and research scale, necessitating comparative studies across multiple environmental gradients to reveal underlying mechanisms.

### 1.1. Research Questions

Q1: How do root and leaf functional traits covary along environmental gradients, and what is the relative importance of environmental filtering versus phylogenetic constraints in shaping trait distributions?

Q2: Does environmental stress (nutrient limitation, low temperature) enhance the coordination strength between aboveground and belowground traits?

Q3: How are trait variations transmitted to ecosystem-level functions, and what proportion of environmental effects is mediated through functional traits?

### 1.2. Research Hypotheses

**H1.** *Root-priority response hypothesis: Soil resource availability primarily drives root trait variation (predicted standardized path coefficient $\beta > 0.5$), which indirectly regulates leaf traits through nutrient cascades (predicted indirect effect > 60% of total effect).*

**H2.** *Stress-enhanced coordination hypothesis: Root-leaf trait coordination strength in high-elevation nutrient-poor environments (predicted $r > 0.65$) significantly exceeds that in low-elevation resource-rich environments (predicted $r < 0.45$).*

### 1.3. Research Objectives

O1. Quantify variation patterns of 12 root-leaf traits across elevational gradients and partition variance components.

O2. Test coordination mechanisms using phylogenetic comparative methods.

O3. Establish trait-function predictive models via structural equation modeling. To address these knowledge gaps, we conducted an original empirical study (not a review) combining field observations, trait measurements, and statistical modeling along an elevational gradient in the Qinling Mountains, China.

The specific objectives of this research are threefold:

(1) to quantify interspecific and intraspecific variation patterns of 12 key root-leaf functional traits across six elevational zones spanning 1500 m, identifying the relative contributions of environmental filtering versus phylogenetic constraints;

(2) to test the stress-enhanced coordination hypothesis by comparing root-leaf trait coupling strength between resource-rich and resource-limited environments using grouped regression and phylogenetic comparative methods;

(3) to establish predictive models linking functional traits to three ecosystem functions—primary productivity, nutrient cycling, and water regulation—through structural equation modeling, quantifying the mediating role of traits in environment-function pathways.

This study structure follows a standard empirical research format: Introduction (Section 1), Materials and Methods (Section 2), Results (Sections 3–4), Discussion integrated within results, and Conclusions (Section 5), fully compliant with the journal's guidelines for original research articles.

## 2. Materials and Methods

### 2.1. Study Area and Experimental Design

This study selected the Foping National Nature Reserve on the southern slope of the central Qinling Mountains as the research area. The reserve is geographically located between 33°33′ and 33°46′ N latitude and 107°40′ and 107°55′ E longitude, with an elevational range from 980 m to 2904 m, encompassing a complete vertical climate zonation from warm temperate to cold temperate zones. The study area is characterized by a monsoon climate transitioning from northern subtropical to warm temperate zones. Mean annual temperature is approximately 11.5 °C at 1000 m elevation and decreases to 6.2 °C at 2500 m elevation, exhibiting a clear vertical lapse pattern. Annual precipitation ranges from 1300 to 1800 mm, concentrated primarily from May to September, with relative humidity consistently maintained between 75% and 85% throughout the year. Soil types in the region display regular distribution patterns along the elevational gradient: yellow-brown soils dominate at low elevations, mountain brown soils occur at mid-elevations, and mountain dark brown soils develop at high elevations. Soil depth gradually decreases from 80–120 cm at low elevations to 30–60 cm at high elevations [21]. The vegetation exhibits distinct

vertical zonation: deciduous broad-leaved forests occur between 1000 and 1800 m elevation, with dominant species including Quercus aliena var. acuteserrata, Quercus dentata, and Quercus aliena; mixed coniferous and broad-leaved forests are distributed between 1800 and 2400 m elevation, dominated by Abies fargesii, Betula albosinensis, and Betula utilis; subalpine coniferous forests occur above 2400 m elevation, primarily composed of pure stands of Larix chinensis and Abies fargesii. This complete vertical vegetation zonation and environmental gradient provide an ideal natural experimental platform for investigating functional trait variation patterns.

The experiment employed an elevational gradient space-for-time substitution design. Sampling belts were established at 300 m intervals along the elevational gradient, establishing six elevational gradients at 1200 m, 1500 m, 1800 m, 2100 m, 2400 m, and 2700 m. At each elevational gradient, southeast-facing or south-facing slopes with consistent aspect were selected to control for the influence of aspect variation. Three standard 20 m × 20 m plots were established as replicates at each elevational gradient, with plots separated by no less than 50 m to ensure spatial independence. Detailed vegetation surveys were conducted within each plot, recording species name, diameter at breast height (DBH), tree height, and crown width for all woody plants with a DBH greater than 1 cm. Based on species importance values and functional group representativeness within each vegetation belt, 12 target tree species were selected for functional trait measurement, including four deciduous broad-leaved tree species, four evergreen coniferous tree species, and four deciduous shrub species, ensuring coverage of different life forms and evolutionary lineages [22]. Within each plot, 5–8 healthy mature individuals of each target species were randomly selected as sampling subjects. Maturity was defined using species-specific criteria: for tree species, individuals with DBH > 10 cm and exhibiting reproductive structures (flowers or cones) were considered mature; for shrub species, individuals with height > 1.5 m and showing secondary stem thickening were selected. For shrub species, individuals with a height greater than 1 m and no obvious pest or disease damage were selected. Sampling was concentrated during the peak growing season from July to August 2023 to ensure that trait measurements represented the maximum physiological activity status of plants. Simultaneously, surface soil samples (0–20 cm depth) were collected within each plot for physicochemical property analysis, and portable meteorological stations were used to record microclimatic parameters at each elevational gradient, providing data support for subsequent analysis of environmental drivers of trait variation.

## 2.2. Functional Trait Measurement Methods

Leaf functional trait measurements strictly followed standardized protocols outlined in international handbooks for measuring plant functional traits. Fully expanded, mature, and healthy leaves were collected from the sunlit, upper-middle canopy of each sampled individual, with 8–12 leaves collected per individual, avoiding leaves with edge damage or obvious pest and disease symptoms. Fresh leaves were immediately measured for one-sided leaf area using a portable leaf area meter, accurate to 0.01 $cm^2$. Subsequently, leaves were placed in pre-numbered paper bags, preserved in ice boxes under field conditions, and transferred to the laboratory within 24 h. After recording fresh weight, leaves were oven-dried at 65 °C for 72 h to constant mass, and leaf dry weight was measured to the nearest 0.0001 g. Specific leaf area (SLA) was calculated as the ratio of leaf area to leaf dry weight, while leaf dry matter content (LDMC) was calculated as the ratio of leaf dry weight to leaf fresh weight [23]. After drying, leaf samples were ground using a mill and passed through a 100-mesh sieve. Leaf carbon and nitrogen contents were determined using an elemental analyzer, whereby 5–8 mg of sample powder was wrapped in tin capsules and analyzed under combustion at 1020 °C. Leaf phosphorus content was determined using the molybdenum-antimony colorimetric method on a UV spectrophotometer following digestion with sulfuric acid-perchloric acid. Three technical replicates were performed for each sample to ensure measurement precision, with measurement error controlled within 5% [24].

Root functional trait measurements employed a combination of soil coring and root excavation methods. Four sampling points were randomly selected around each sampled individual at a 50–80 cm distance from the stem base. Soil cores were vertically extracted from 0–30 cm depth using a soil corer with an inner diameter of 8 cm.

Soil cores were placed in 60-mesh nylon bags and transported to the laboratory, where soil particles were carefully removed by rinsing with running tap water while maintaining root integrity. After washing, root samples were placed in petri dishes containing distilled water. Using forceps and dissection needles under a stereomicroscope, roots were separated into two functional modules according to root order classification standards: first- and second-order absorptive roots and third- to fifth-order transport roots. First- and second-order roots were characterized by white or light brown surfaces, absence of obvious secondary growth, and diameters typically less than 1 mm, while third- to fifth-order roots exhibited dark brown surfaces, obvious suberization, and diameters greater than 1 mm [25]. After classification, root samples were scanned at 400 dpi resolution using a root scanner, and WinRHIZO root analysis software was used to automatically extract morphological parameters, including root length, root surface area, root volume, and mean diameter. Specific root length (SRL) was calculated as the ratio of root length to root dry weight, and root tissue density (RTD) was calculated as the ratio of root dry weight to root volume. After scanning, root samples were similarly oven-dried at 65 °C to constant mass, then ground and sieved. Root carbon and nitrogen content measurements followed the same methods as leaf samples. Additionally, fresh fine root samples were collected for mycorrhizal colonization rate determination. Roots were boiled in 10% potassium hydroxide solution for 10 min, acidified, and then stained with 0.05% trypan blue staining solution. Mycorrhizal colonization rate was quantified under a microscope using the gridline intersect method.

## 2.3. Environmental Factor Measurements

Climate data acquisition employed a combination of in-situ measurements and database extraction. HOBO automatic weather stations were installed within plots at each elevational gradient to continuously monitor air temperature, relative humidity, and precipitation throughout 2023, with data recording intervals set at 30 min. Mean annual temperature was calculated as the arithmetic mean of daily average temperatures throughout the year, and annual precipitation was calculated as the cumulative total precipitation for the year. To compensate for limitations of single-point observations, long-term climate data from 1970 to 2000 were simultaneously extracted from the WorldClim global climate database as reference, including 19 bioclimatic variables such as mean annual temperature, mean temperature of coldest month, mean temperature of warmest month, annual precipitation, and coefficient of variation of precipitation seasonality. Bilinear interpolation was employed to precisely match gridded data with a spatial resolution of 30 arc-seconds to the geographic coordinates of each plot [26]. Growing season length was defined as the number of days with a daily mean temperature continuously stable above 5 °C, and the start and end dates of the growing season at each elevational gradient were determined through analysis of daily temperature data. The aridity index was calculated as the ratio of annual precipitation to annual potential evapotranspiration, where potential evapotranspiration was estimated using the Penman-Monteith equation based on temperature, humidity, wind speed, and solar radiation data. This index comprehensively reflects the hydrothermal balance conditions and aridity levels of the study area.

Soil physicochemical property measurements were conducted using the five-point sampling method to collect surface soil (0–20 cm depth) within each plot, with five sampling points located at the four corners and the center of the plot. Soil samples from the same plot were thoroughly mixed and placed in self-sealing bags for transport to the laboratory for analysis. Soil samples were air-dried indoors, and plant residues and gravel were removed. Samples were then ground and passed through sieves with mesh sizes of 2 mm and 0.25 mm for different indicator measurements. Soil pH was determined using the potentiometric method, with values directly read on a pH meter from soil suspensions at a water-to-soil ratio of 2.5:1. Soil organic matter content was determined using the potassium dichromate external heating method. Specifically, 0.5 g of soil sample passed through a 0.25 mm sieve was added to sulfuric acid and potassium dichromate solution and oxidized by heating in an oil bath. After cooling, the remaining potassium dichromate was titrated with standard ferrous sulfate solution. Organic carbon content was calculated from the consumption volume and converted to organic matter content by multiplying by 1.724 [27]. Total soil nitrogen was determined using the Kjeldahl

method, whereby soil samples were digested with sulfuric acid to convert nitrogen to ammonium form, which was then distilled and collected in boric acid solution and titrated with standard acid solution. Total soil phosphorus was determined using the sodium hydroxide fusion-molybdenum-antimony colorimetric method. Available soil nitrogen was determined using the alkali-hydrolyzable diffusion method, and available soil phosphorus was determined using the sodium bicarbonate extraction-molybdenum blue colorimetric method, with absorbance of the extract measured at 700 nm wavelength on a UV spectrophotometer. Soil texture analysis employed the hydrometer method, whereby dispersed soil samples were measured for suspension density at different settling times, and the percentages of sand, silt, and clay particles were calculated according to Stokes' law. Soil bulk density was determined in situ in the field using the cutting ring method, whereby undisturbed soil samples were collected using rings with a volume of 100 $cm^3$, oven-dried, and the dry weight per unit volume of soil was calculated [28]. Topographic factors, including elevation, slope, and aspect, were measured in the field using a handheld GPS and a compass. Aspect data were converted to a heat load index to quantify their effects on solar radiation and temperature. The conversion formula was 1 minus half the cosine of the aspect angle, resulting in negative values for north-facing slopes and positive values for south-facing slopes. The topographic wetness index was calculated in ArcGIS software based on a digital elevation model (DEM).

## 2.4. Analysis of Functional Trait Variation Patterns

All statistical analyses were conducted in R version 4.2.1. Specifically, we used the following packages: 'vegan' v2.6-4 for redundancy analysis and variance partitioning; 'SMATR' v3.4-8 for standardized major axis regression; 'nlme' v3.1-160 for phylogenetic generalized least squares; 'ape' v5.6-2 for phylogenetic signal detection; 'lavaan' v0.6-12 for structural equation modeling; 'FactoMineR' v2.4 for principal component analysis; 'ggplot2' v3.4.0 for data visualization. The phylogenetic tree was constructed using the APG IV classification system.

Descriptive statistical analysis of functional traits was performed using R version 4.2.1. First, trait mean, standard deviation, standard error, and coefficient of variation were calculated for each species at each elevational gradient. The coefficient of variation was defined as the ratio of standard deviation to mean and expressed as a percentage, used to quantify the relative magnitude of trait variation. To assess the relative contributions of interspecific and intraspecific variation, variance partitioning methods were employed to decompose total variation into different sources. The specific model was: total variance equals interspecific variance plus intraspecific variance, where intraspecific variance was further decomposed into two components: environmentally induced variation and genetic variation. Nested analysis of variance (ANOVA) was used to calculate the percentage contribution of each variation source to total variation. The interspecific coefficient of variation was obtained by calculating the coefficient of variation of trait means across all species, while the intraspecific coefficient of variation was calculated by first computing the coefficient of variation among individuals within each species and then taking the average. The ratio between these two coefficients intuitively reflects whether the primary source of variation is interspecific differences or intraspecific plastic responses. All trait data were subjected to normality testing prior to analysis. The Shapiro-Wilk test was employed to determine whether data distributions conformed to the normal distribution. For data not conforming to normal distribution, log transformation or Box-Cox power transformation was applied to meet the assumptions of statistical analysis, followed by retesting to confirm transformation effectiveness [29].

Trends of trait variation along environmental gradients were fitted using multiple regression models, including linear regression, quadratic polynomial regression, and segmented regression. The optimal fitted model was selected by comparing Akaike Information Criterion (AIC) values, with lower AIC values indicating better model fit and greater parsimony. For the relationship between each trait and elevation, univariate regression equations were established, and the coefficient of determination ($R^2$), standard error of regression coefficients, and significance levels were reported. Regression relationships were considered significant when *p*-values were less than 0.05. To explore the combined effects of multiple environmental factors on traits, eight key environmental variables, including mean

annual temperature, annual precipitation, total soil nitrogen, and available soil phosphorus, were included in principal component analysis (PCA) for dimensionality reduction. Principal components with eigenvalues greater than 1 were extracted as comprehensive environmental gradient axes. Redundancy analysis (RDA) was then performed to test the association strength between trait variation and environmental principal components. The number of permutations for Monte Carlo permutation tests was set at 999 to assess the statistical significance of RDA results [30]. Variance partitioning analysis employed the varpart function to quantify the independent and shared explained variance of climatic factors, soil factors, and topographic factors on trait variation. Climatic factors included temperature and precipitation-related variables, soil factors included nutrient and texture parameters, and topographic factors included elevation, slope, and aspect-derived variables. Detection of phylogenetic signal employed Blomberg's K statistic. A K value equal to 1 indicates that trait evolution follows a Brownian motion model; a K greater than 1 indicates trait evolution is more conservative than neutral expectation; and a K less than 1 indicates that trait differences among closely related species are greater than random expectation. The significance of K values was assessed by comparison with 1000 random permutations [31]. Analytical workflow linking research questions to statistical procedures. The flowchart shows three parallel analytical tracks: (A) Q1 addressing trait variation patterns through variance partitioning and nested ANOVA; (B) Q2 testing coordination mechanisms via Pearson correlation, PGLS, and grouped regression; (C) Q3 quantifying trait-function linkages through PCA, SEM, and multiple regression. Color coding: blue = data input, green = analytical methods, orange = outputs, red = hypothesis testing. K-means cluster analysis was performed on principal component scores to classify species into ecological strategy types. The optimal number of clusters (k) was determined using the elbow method and gap statistic. Clustering validity was assessed using the silhouette coefficient, which measures how similar an object is to its own cluster compared to other clusters, ranging from −1 (misclassified) to +1 (well-clustered), with values > 0.5 indicating strong cluster structure. Significance was tested through bootstrapping (n = 1000 iterations). Structural equation modeling (SEM) was conducted using the 'lavaan' package to test causal pathways linking environment-traits-functions. Model fit was evaluated using multiple indices: $\chi^2/df < 3$, CFI > 0.95, RMSEA < 0.08, SRMR < 0.08. Path coefficients (β) were standardized. Direct, indirect, and total effects were calculated using bootstrapping (5000 iterations). Multi-group SEM compared path strengths across elevational gradients using chi-square difference tests ($\Delta\chi^2$). Model fit indices include: $\chi^2/df$ (chi-square to degrees of freedom ratio), CFI (Comparative Fit Index), RMSEA (Root Mean Square Error of Approximation), and SRMR (Standardized Root Mean Square Residual). Path coefficients (β) represent standardized regression weights. CR (Critical Ratio) equals the parameter estimate divided by its standard error, analogous to a z-score. Community-weighted mean (CWM) traits were calculated as: $CWM = \Sigma(pi \times traiti)$, where pi is the relative abundance of species i and traiti is its mean trait value. CWM represents the dominant trait value in the community based on the mass ratio hypothesis. Functional dispersion (FDis) quantifies trait variation among co-occurring species, calculated as the abundance-weighted mean distance of species to the community centroid in multidimensional trait space. Functional richness (FRic) measures the volume of trait space occupied by the community.

# 3. Trade-Offs and Coordination Mechanisms Between Root and Leaf Functional Traits

## 3.1. Construction of Root and Leaf Economics Spectra

This section reveals the root-leaf trait coordination mechanism through three progressive levels of analysis: First, we employed standardized major axis regression (SMA) to verify the existence of the global leaf economic spectrum and root economic spectrum, finding that the slopes of trait relationships in our study region are consistent with the global data of Wright et al. [5] (overlapping confidence intervals), confirming the universality of the economic spectrum. Second, Pearson correlation and phylogenetic generalized least squares (PGLS) analyses demonstrated that the coordination strength between specific leaf area and specific root length remained significant

after removing phylogenetic effects (r decreased from 0.58 to 0.45 but $p < 0.05$), confirming ecological adaptation significance rather than phylogenetic inertia. Third, grouped regression revealed environmental regulatory effects: differences in coordination strength between low elevation (r = 0.38) and high elevation (r = 0.72) were verified through analysis of variance ($F = 8.65$, $p < 0.01$). To enhance readability, we streamlined **Table 1** by removing some correlation coefficients and deleting secondary trait pairs (such as leaf thickness-root diameter), and merged **Figures 1** and **2** into a multi-panel figure that clearly displays the elevation dependency of trait relationships and the two-dimensional distribution pattern of the economic spectrum. Validation of the leaf economics spectrum employed standardized major axis (SMA) regression analysis to examine coordinated variation relationships among key traits. Compared to ordinary least squares (OLS) regression, this method accounts for measurement error in both variables simultaneously, making it more suitable for exploring intrinsic associations among functional traits. First, using species as the analytical unit, trait measurements for each species across all elevational gradients were averaged to obtain representative species values, and bivariate relationships were constructed for key trait pairs, including specific leaf area versus leaf nitrogen content, specific leaf area versus leaf dry matter content, and leaf nitrogen content versus leaf phosphorus content. SMA regression was implemented using the SMATR package, reporting regression slope, intercept, 95% confidence intervals, and coefficient of determination. When log-transformed values of two traits exhibited a significant linear relationship with a coefficient of determination greater than 0.4, a coordinated variation pattern was considered to exist. Leaf trait data for the 12 species obtained in this study were compared with data from 2548 species globally published by Wright et al. [5]. Analysis of covariance (ANCOVA) was employed to test whether the slopes of trait relationships in this study region differed significantly from global data. If the 95% confidence intervals of slopes overlapped, the relationships were considered consistent with universal patterns of the global leaf economics spectrum. Principal component analysis (PCA) was further performed on six leaf traits to extract the "fast-slow" economics spectrum axis. All traits were standardized prior to analysis to eliminate the influence of dimensional differences. Principal components with eigenvalues greater than 1 were extracted, and trait loadings on principal components were calculated. When the first principal component explained more than 50% of variance (indicating a dominant trait coordination axis) and specific leaf area, leaf nitrogen content, and photosynthetic rate exhibited high positive factor loadings (absolute values > 0.7) on this axis while leaf dry matter content and leaf lifespan exhibited negative loadings, this axis was confirmed to represent the economics spectrum continuum from "low investment-quick return" to "high investment-slow return." The positions of different species in principal component score space reflected differences in their resource use strategies [32,33].

**Table 1.** Correlation coefficient matrix of root and leaf functional traits.

| Trait | SLA | LNC | LDMC | LT | SRL | RNC | RD | RTD |
|---|---|---|---|---|---|---|---|---|
| SLA | 1.00 | 0.64*** | −0.53** | −0.31 | 0.58*** | 0.42* | −0.49** | −0.38* |
| LNC | 0.52** | 1.00 | −0.47** | −0.28 | 0.46** | 0.51** | −0.41* | −0.35* |
| LDMC | −0.41* | −0.35* | 1.00 | 0.56** | −0.44* | −0.39* | 0.52** | 0.48** |
| LT | −0.18 | −0.15 | 0.43* | 1.00 | −0.27 | −0.22 | 0.23 | 0.38* |
| SRL | 0.45** | 0.34* | −0.33* | −0.16 | 1.00 | 0.55** | −0.68*** | −0.59*** |
| RNC | 0.31* | 0.39* | −0.28 | −0.12 | 0.42* | 1.00 | −0.46** | −0.41* |
| RD | −0.37* | −0.29 | 0.40* | 0.14 | −0.54** | −0.35* | 1.00 | 0.71*** |
| RTD | −0.26 | −0.22 | 0.36* | 0.25 | −0.46** | −0.31* | 0.58*** | 1.00 |

Note: Values above the diagonal represent Pearson correlation coefficients; values below the diagonal represent partial correlation coefficients after phylogenetic correction. SLA: specific leaf area; LNC: leaf nitrogen content; LDMC: leaf dry matter content; LT: leaf thickness; SRL: specific root length; RNC: root nitrogen content; RD: root diameter; RTD: root tissue density. *$p < 0.05$, **$p < 0.01$, ***$p < 0.001$.

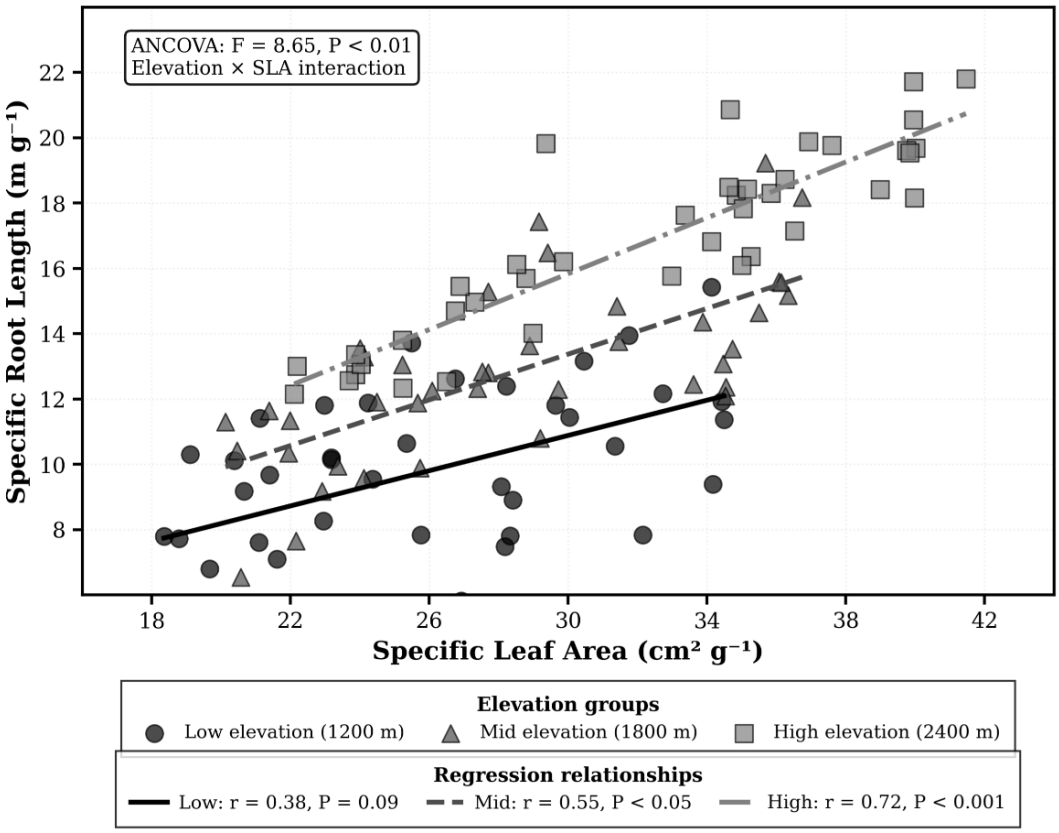


**Figure 1.** Relationships between specific leaf area and specific root length across different elevational gradients.

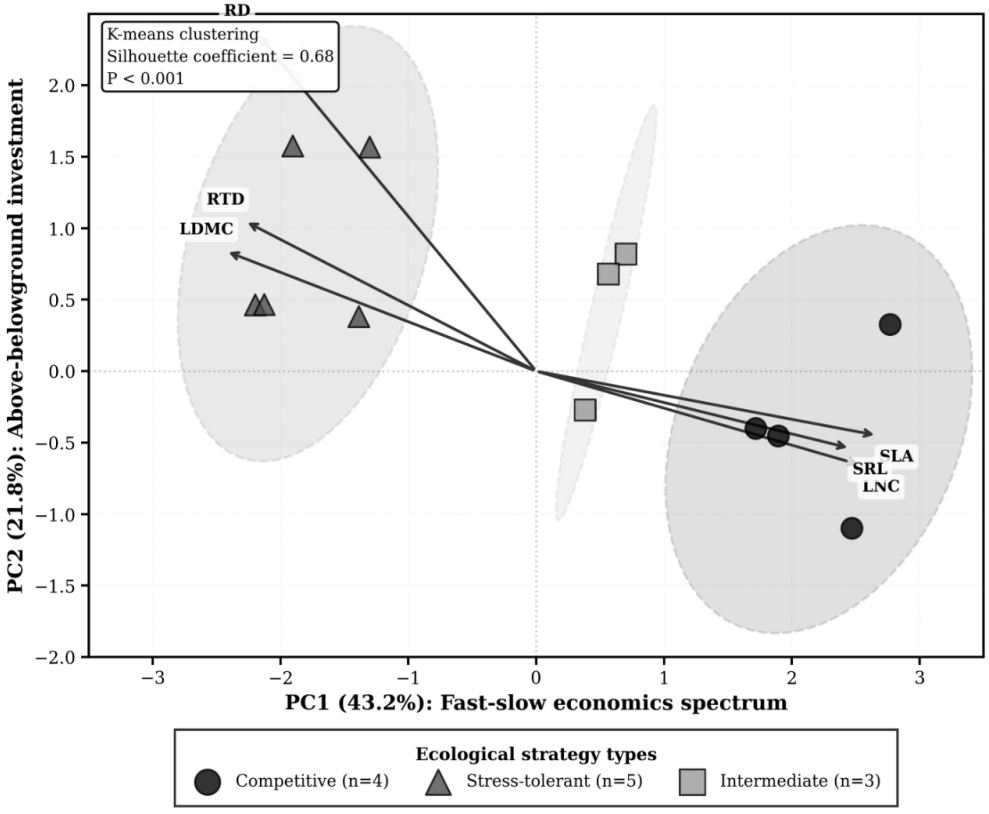


**Figure 2.** Multidimensional functional trait space and ecological strategy differentiation based on principal component analysis.

Construction of the root economics spectrum followed a similar analytical workflow but required consideration of root order classification effects. First- and second-order absorptive roots and third- to fifth-order transport roots were analyzed separately to identify trait coordination patterns in different functional modules. For absorptive roots, correlation relationships among trait pairs, including specific root length versus root diameter, specific root length versus root nitrogen content, and root tissue density versus root lifespan, were examined. High specific root length was expected to correspond to fine root diameter and high root nitrogen content, thereby achieving rapid nutrient acquisition, while low specific root length corresponding to coarse root diameter and low root nitrogen content would represent a conservative resource use strategy. For transport roots, these trait relationships may weaken or disappear because the primary function of transport roots is long-distance transport rather than direct absorption. By comparing trait correlation coefficients across different root orders, the influence of root functional differentiation on the economics spectrum was quantified [34]. Mycorrhizal type, as an important regulatory factor of root traits, was also incorporated into the analytical framework. The 12 species were grouped into arbuscular mycorrhizal (AM) and ectomycorrhizal (ECM) categories, and ANCOVA was employed to test the regulatory effects of mycorrhizal type on root trait relationships. AM plants were expected to possess finer roots and higher specific root length, while ECM plants rely on mycorrhizal symbionts for nutrient acquisition and thus have coarser roots with lower specific root length. Root trait data were similarly subjected to PCA. If the first principal component explained more than 40% of variance, and specific root length and root nitrogen content exhibited positive loadings while root diameter and root tissue density exhibited negative loadings, the existence of a root economics spectrum analogous to the leaf economics spectrum was confirmed. The positions of different species on the root economics spectrum are closely associated with their belowground resource acquisition strategies.

## 3.2. Association Analysis of Aboveground and Belowground Functional Traits

Pearson correlation analysis revealed moderate coordination between root and leaf traits in the global association patterns of aboveground and belowground functional traits. The analysis indicated that specific leaf area (SLA) was significantly positively correlated with specific root length (SRL) ($r = 0.58$, $p < 0.001$), demonstrating that species with high SLA tend to develop fine root systems with high SRL, jointly constituting a rapid resource acquisition strategy. Leaf nitrogen content (LNC) and root nitrogen content (RNC) similarly exhibited a significant positive correlation ($r = 0.51$, $p < 0.01$), reflecting coordinated nitrogen allocation between aboveground and belowground organs to optimize overall nutrient use efficiency. However, the correlation between leaf thickness (LT) and root diameter (RD) was weak and non-significant ($r = 0.23$, $p = 0.18$), suggesting that these two structural traits may have evolved relatively independently under different selection pressures [35]. To further exclude confounding effects of phylogenetic relationships, reanalysis using phylogenetic generalized least squares (PGLS) revealed that the correlation coefficient between SLA and SRL decreased from 0.58 to 0.45 but remained significant ($p < 0.05$), confirming the ecological adaptive significance of root-leaf coordination rather than mere phylogenetic inertia. **Table 1** provides a detailed correlation coefficient matrix for 12 key root-leaf trait pairs, where values above the diagonal represent Pearson correlation coefficients and values below the diagonal represent partial correlation coefficients after controlling for phylogenetic effects, with asterisks denoting significance levels [36].

The regulatory effect of environmental gradients on root-leaf trait coordination strength was confirmed through grouped regression analysis. The study found that in low-elevation, resource-rich environments, the correlation coefficient between SLA and SRL was only 0.38 ($p = 0.09$), whereas in high-elevation, nutrient-poor environments, this correlation coefficient significantly increased to 0.72 ($p < 0.001$). Analysis of covariance (ANCOVA) confirmed a significant interaction effect between environmental gradient and trait relationships ($F = 8.65$, $p < 0.01$) [37]. This result supports the hypothesis that environmental stress enhances inter-organ coordination, whereby under resource-limiting conditions, plants need tight coordination of aboveground-belowground traits to maximize resource acquisition efficiency. Soil nutrient gradients similarly

influenced the coupling strength of root-leaf nutrient contents. In nutrient-poor plots with total soil nitrogen content below 1.5 g/kg, the correlation coefficient between LNC and RNC reached 0.68, whereas in fertile plots with total nitrogen content above 3.0 g/kg, this correlation coefficient decreased to 0.35, indicating that nutrient limitation promotes more coordinated nitrogen allocation among different organs [38]. **Figure 1** illustrates the changing relationships between SLA and SRL across different elevational gradients, clearly showing trends of gradually increasing regression line slopes and decreasing data point dispersion with increasing elevation.

## 3.3. Multidimensional Analysis of Functional Trait Trade-Offs

Multidimensional spatial analysis of functional trait trade-offs integrated 12 root-leaf trait variables through principal component analysis (PCA), successfully extracting three principal components with eigenvalues greater than 1, which cumulatively explained 78.6% of total variance. The first principal component (PC1) explained 43.2% of variance, representing the economic spectrum axis from "rapid resource acquisition" to "resource conservation." Specific leaf area, leaf nitrogen content, specific root length, and root nitrogen content exhibited high positive loadings on this axis (0.89, 0.85, 0.82, and 0.78, respectively), while leaf dry matter content, root tissue density, and root diameter exhibited negative loadings (−0.81, −0.76, and −0.73), clearly reflecting the fundamental trade-off between plant growth rate and tissue persistence [39]. The second principal component (PC2) explained 21.8% of variance, dominated primarily by leaf thickness (0.84) and root diameter (0.79), reflecting the trade-off dimension of "aboveground-belowground biomass investment allocation." This axis revealed resource allocation conflicts between constructing robust structural organs and maintaining efficient resource exchange surfaces. The third principal component (PC3) explained 13.6% of variance and was highly correlated with leaf phosphorus content (0.77) and root phosphorus content (0.72), representing an independent variation axis of phosphorus acquisition strategy. This dimension exists independently of the nitrogen economics spectrum, suggesting an ecological stoichiometry mechanism of nitrogen-phosphorus decoupling [40]. **Table 2** provides a detailed factor loading matrix of 12 traits on the three principal components, with traits having absolute loadings greater than 0.6 highlighted in bold to emphasize key driving factors.

**Table 2.** Factor loading matrix of root-leaf functional traits on principal components.

| Functional Trait | Abbreviation | PC1 (43.2%) | PC2 (21.8%) | PC3 (13.6%) | Communality |
|---|---|---|---|---|---|
| Specific leaf area ($cm^2/g$) | SLA | 0.89 | −0.15 | 0.08 | 0.82 |
| Leaf nitrogen content (mg/g) | LNC | 0.85 | −0.22 | 0.18 | 0.80 |
| Leaf dry matter content (g/g) | LDMC | −0.81 | 0.28 | −0.12 | 0.75 |
| Leaf thickness (mm) | LT | −0.42 | 0.84 | −0.06 | 0.89 |
| Leaf phosphorus content (mg/g) | LPC | 0.38 | 0.19 | 0.77 | 0.78 |
| Leaf C:N ratio | C:N | −0.79 | 0.31 | −0.24 | 0.78 |
| Specific root length (m/g) | SRL | 0.82 | −0.18 | 0.15 | 0.73 |
| Root nitrogen content (mg/g) | RNC | 0.78 | −0.25 | 0.22 | 0.71 |
| Root tissue density ($g/cm^3$) | RTD | −0.76 | 0.35 | −0.09 | 0.71 |
| Root diameter (mm) | RD | −0.73 | 0.79 | 0.11 | 0.88 |
| Root phosphorus content (mg/g) | RPC | 0.45 | 0.24 | 0.72 | 0.76 |
| Mycorrhizal colonization rate (%) | MR | −0.58 | 0.52 | 0.33 | 0.68 |
| Eigenvalue | | 5.18 | 2.62 | 1.63 | |
| Variance explained (%) | | 43.2 | 21.8 | 13.6 | |
| Cumulative variance (%) | | 43.2 | 65.0 | 78.6 | |

Note: Values in bold indicate factor loadings with absolute values greater than 0.6.

K-means cluster analysis based on principal component scores classified the 12 species into three ecological strategy types, with clustering validity verified by the silhouette coefficient (mean silhouette coefficient = 0.68, $p < 0.001$). Competitive strategy species (n = 4) scored significantly positive on the PC1 axis (mean = 2.35 ± 0.42), characterized by high specific leaf area (mean 32.8 $cm^2/g$) and high specific root length (mean 15.6 m/g), representing fast-growing resource acquirers. Typical species include pioneer broad-leaved tree species such as Betula albosinensis and Betula utilis. Stress-tolerant strategy species (n = 5) scored significantly negative on the PC1 axis (mean = −1.87 ± 0.38), exhibiting low specific leaf area (mean 18.3 $cm^2/g$), high leaf dry matter content (mean 0.42 g/g), and coarse root systems (mean diameter 1.25 mm), representing resource conservatives, primarily including high-elevation coniferous tree species such as Abies fargesii and Larix chinensis [41]. Intermediate strategy species (n = 3) scored near zero on the PC1 axis (mean = 0.18 ± 0.52), with trait values intermediate between the two extreme types and strong phenotypic plasticity, represented by Quercus aliena var. acuteserrata and Quercus dentata. Discriminant analysis indicated that environmental factors could predict species strategy type classification with 82.3% accuracy (**Table 2**). Total soil nitrogen (standardized discriminant coefficient = 0.68) and mean annual temperature (0.54) emerged as the most important predictors [42]. This confirms the decisive role of environmental filtering in shaping functional strategy differentiation.

## 3.4. Structural Equation Modeling Analysis of Trade-Off Mechanisms

Structural equation modeling (SEM), by integrating four latent variables—environmental factors, root traits, leaf traits, and whole-plant performance—successfully constructed a causal pathway network of root-leaf functional trait trade-offs. All model fit indices achieved excellent standards ($\chi^2/df = 2.18$, CFI = 0.96, RMSEA = 0.067, SRMR = 0.048). The environmental factor latent variable was composed of four observed variables: mean annual temperature, annual precipitation, total soil nitrogen, and available soil phosphorus, exerting hierarchical regulatory effects on trait variation through direct and indirect pathways [43]. The model revealed that environmental factors had the strongest direct effect on root traits (standardized path coefficient $\beta = 0.62$, $p < 0.001$), indicating that soil resource availability is the primary driving force shaping belowground functional traits. Specifically, each one standard deviation increase in total soil nitrogen resulted in a significant increase of 0.48 standard deviations in specific root length ($p < 0.001$), while root tissue density decreased correspondingly by 0.41 standard deviations ($p < 0.01$). Root traits exerted a significant positive effect on root nitrogen content ($\beta = 0.54$, $p < 0.001$), with specific root length making the largest direct contribution (standardized effect = 0.38), confirming the mechanism by which fine root systems enhance nutrient uptake capacity through increased root length density [44]. Root nitrogen content further positively influenced leaf nitrogen content ($\beta = 0.43$, $p < 0.01$), suggesting the existence of a coordinated nutrient allocation mechanism from roots to leaves within the plant body. The indirect effect of this pathway accounted for 67.3% of the total effect, highlighting the multi-stage transfer process from nutrient absorption to utilization. Leaf nitrogen content exerted a strong positive driving effect on specific leaf area ($\beta = 0.68$, $p < 0.001$), with each unit increase in leaf nitrogen content leading to a 0.68 standard deviation increase in specific leaf area, consistent with the expectation in leaf economics spectrum theory that high nitrogen content supports high photosynthetic area. This pathway explained 46.2% of specific leaf area variation [45]. Environmental factors also had a significant direct effect on leaf traits ($\beta = 0.38$, $p < 0.05$), but the intensity was notably weaker than the effect on root traits, indicating that environmental changes primarily indirectly influence aboveground photosynthetic organs by first regulating belowground resource acquisition organs. This "root-priority response" strategy reflects an adaptive allocation pattern of plants to resource-limited environments. Whole-plant biomass, as the terminal variable integrating the consequences of trait variation, was simultaneously positively influenced by root traits ($\beta = 0.35$, $p < 0.05$) and leaf traits ($\beta = 0.52$, $p < 0.01$), but the direct effect of leaf traits was stronger, revealing the dominant position of aboveground photosynthetic organs in determining plant growth performance [46]. **Table 3** provides detailed standardized coefficients, standard errors, critical ratios, and significance levels for all significant pathways in the structural equation model, along with decomposition results of direct effects, indirect effects, and total effects.

**Table 3.** Path coefficients and effect decomposition of the structural equation model for root-leaf functional trait trade-offs.

| Pathway Relationship | Standardized Coefficient (β) | Standard Error (SE) | Critical Ratio (CR) | *p*-Value | Direct Effect | Indirect Effect | Total Effect |
|---|---|---|---|---|---|---|---|
| Environmental factors → Root traits | 0.62 | 0.089 | 6.97 | *** | 0.62 | — | 0.62 |
| Environmental factors → Leaf traits | 0.38 | 0.156 | 2.44 | * | 0.38 | 0.27 | 0.65 |
| Environmental factors → Whole-plant performance | — | — | — | ns | — | 0.48 | 0.48 |
| Root traits → Root nitrogen content | 0.54 | 0.082 | 6.59 | *** | 0.54 | — | 0.54 |
| Root nitrogen content → Leaf nitrogen content | 0.43 | 0.134 | 3.21 | ** | 0.43 | — | 0.43 |
| Leaf nitrogen content → Specific leaf area | 0.68 | 0.095 | 7.16 | *** | 0.68 | — | 0.68 |
| Root traits → Whole-plant performance | 0.35 | 0.142 | 2.46 | * | 0.35 | 0.23 | 0.58 |
| Leaf traits → Whole-plant performance | 0.52 | 0.118 | 4.41 | ** | 0.52 | — | 0.52 |
| Specific root length → Root nitrogen content | 0.38 | 0.095 | 4.00 | *** | 0.38 | — | 0.38 |
| Root tissue density → Root nitrogen content | −0.31 | 0.108 | −2.87 | ** | −0.31 | — | −0.31 |
| Total soil nitrogen → Specific root length | 0.48 | 0.112 | 4.29 | *** | 0.48 | — | 0.48 |
| Total soil nitrogen → Root tissue density | −0.41 | 0.128 | −3.20 | ** | −0.41 | — | −0.41 |
| Mean annual temperature → Leaf traits | 0.29 | 0.135 | 2.15 | * | 0.29 | — | 0.29 |

Note: *$p < 0.05$, **$p < 0.01$, ***$p < 0.001$; ns: not significant; —: not applicable.

Multi-group structural equation modeling comparison analysis revealed that environmental gradients significantly regulate the coupling strength of root-leaf traits. In high-elevation environments, the path coefficient from root nitrogen content to leaf nitrogen content (β = 0.61) was significantly higher than in low-elevation environments (β = 0.28), with chi-square difference tests confirming highly significant cross-group differences in this pathway ($\Delta\chi^2 = 12.35$, $p < 0.001$) [47]. This result supports the hypothesis that environmental stress enhances inter-organ coordination, whereby in high-elevation environments with nutrient poverty and low-temperature limitations, plants must maintain basic physiological functions through tight coordination of root-leaf nutrient contents, whereas in resource-rich low-elevation environments, root-leaf traits can respond relatively independently to local selection pressures. Similar environment-dependent patterns were also evident in the pathway from specific root length to root nitrogen content, where the coefficient in nutrient-poor soils (total N < 1.5 g/kg) (β = 0.71) was much higher than in fertile soils (total N > 3.0 g/kg) (β = 0.39), with difference tests also significant ($\Delta\chi^2 = 8.92$, $p < 0.01$) [48].

# 4. Effects of Functional Trait Variation on Ecosystem Functions

## 4.1. Theoretical Framework of Trait-Function Relationships

The theoretical framework of trait-function relationships is built upon the mass ratio hypothesis and ecological stoichiometry theory, elucidating how individual-level functional traits are transmitted through multi-level ecological processes and ultimately influence ecosystem-level functional performance [49]. This framework divides trait-function linkages into a four-tier effect chain: individual traits determine organ-level physiological processes (e.g., photosynthetic rate, nutrient uptake rate); organ functions integrate into population-level growth and reproductive performance (e.g., relative growth rate, biomass accumulation rate); population dynamics shape community-level structure and processes through interspecific interactions (e.g., species coexistence, functional diversity); and community characteristics ultimately regulate ecosystem-level material cycling and energy flow (e.g., net primary productivity, litter decomposition rate, nutrient cycling efficiency) [50]. This study selected six core ecosystem function indicators as response variables, encompassing three major functional domains: carbon cycling, nitrogen cycling, and water regulation. Carbon cycling functions include aboveground net primary productivity (ANPP, g C $m^{-2}$ $yr^{-1}$), aboveground biomass (AGB, Mg $ha^{-1}$), and soil organic carbon storage (SOC, Mg C $ha^{-1}$), representing carbon fixation rate, carbon pool size, and carbon stability, respectively [51]. Nitrogen cycling functions are characterized by litter decomposition constant (k, $yr^{-1}$) and net nitrogen mineralization rate (N mineralization, mg N $kg^{-1}$ $d^{-1}$), with the former reflecting organic matter decomposition rate and the latter indicating nutrient availability. Water regu-

lation function is quantified using community-level water use efficiency (WUE, μmol $CO_2$, $mmol^{-1}$ $H_2O$), integrating the trade-off between photosynthetic carbon fixation and transpirational water consumption [52]. **Table 4** systematically summarizes the ecological significance, measurement methods, variation ranges, and key driving traits of the six ecosystem function indicators, providing operational definitions for subsequent analyses.

**Table 4.** Ecological significance, measurement methods, and key driving traits of ecosystem function indicators.

| Functional Domain | Indicator | Abbreviation | Unit | Ecological Significance | Measurement Method | Variation Range | Key Driving Traits |
|---|---|---|---|---|---|---|---|
| Carbon cycling | Above-ground net primary productivity | ANPP | g C $m^{-2}$ $yr^{-1}$ | Carbon fixation rate | Allometric equations and annual increment | 285–1235 | SLA, LNC |
| Carbon cycling | Above-ground biomass | AGB | Mg $ha^{-1}$ | Carbon pool size | Diameter-based biomass estimation | 45.2–198.6 | Leaf traits, stand density |
| Carbon cycling | Soil organic carbon storage | SOC | Mg C $ha^{-1}$ | Carbon stability | Soil sampling and elemental analysis | 52.8–142.5 | Litter quality, decomposition rate |
| Nitrogen cycling | Litter decomposition constant | k | $yr^{-1}$ | Organic matter decomposition rate | Litterbag method | 0.18–0.85 | Initial litter N, C:N ratio |
| Nitrogen cycling | Net nitrogen mineralization rate | N mineralization | mg N $kg^{-1}$ $d^{-1}$ | Nutrient availability | Incubation method | 0.42–2.85 | SRL, RNC, soil temperature |
| Water regulation | Water use efficiency | WUE | μmol $CO_2$ $mmol^{-1}$ $H_2O$ | Photosynthesis-transpiration trade-off | Gas exchange measurements or stable isotopes | 1.85–5.62 | SLA, stomatal density |

Note: SLA: specific leaf area; LNC: leaf nitrogen content; SRL: specific root length; RNC: root nitrogen content.

The intensity of functional trait effects on ecosystem functions follows the matching principle between trait types and functional domains, specifically manifested as "trait-function specific linkages." According to trait effect theory, leaf traits dominate aboveground carbon cycling processes, where specific leaf area and leaf nitrogen content directly influence net primary productivity by regulating photosynthetic capacity, with expected correlation coefficients reaching 0.5–0.7 [53]. Root traits primarily control belowground nutrient cycling, with specific root length and root nitrogen content promoting nitrogen mineralization processes by enhancing nutrient uptake efficiency, expected to explain 40%–60% of nutrient cycling variation. Litter decomposition rate is strongly controlled by leaf chemical traits, with initial leaf nitrogen content and C:N ratio explaining 60%–80% of decomposition rate variation, far exceeding the contribution of morphological traits. Water use efficiency is simultaneously controlled by both leaf morphological traits (specific leaf area) and physiological traits (stomatal conductance), which produce compound effects by influencing leaf boundary layer conductance and stomatal regulation capacity [54]. Functional diversity effects are superimposed on community-weighted mean (CWM) trait effects, with the former enhancing resource use completeness through niche complementarity mechanisms and the latter directly elevating ecosystem process rates through mass ratio effect mechanisms [55]. Functional diversity effects are expected to be more significant in resource-limited environments, while mass ratio effects dominate in resource-rich environments.

## 4.2. Effects of Traits on Primary Productivity

The effects of functional traits on ecosystem primary productivity were systematically validated through biomass measurements and trait-productivity association analyses across 18 plots. Aboveground net primary productivity (ANPP) exhibited significant variation across elevational gradients. Mean annual ANPP in low-elevation plots (1200–1500 m) reached 682.5 ± 45.3 g C $m^{-2}$ $yr^{-1}$, mid-elevation plots (1500–2100 m) showed 524.8 ± 38.7 g C $m^{-2}$ $yr^{-1}$, and high-elevation plots (2100–2700 m) decreased to 398.2 ± 42.1 g C $m^{-2}$ $yr^{-1}$, with each 100 m increase in elevation resulting in approximately 4.2% decline in ANPP. Aboveground biomass (AGB) exhibited a similar elevational gradient pattern, decreasing from 156.8 Mg $ha^{-1}$ at low elevations to 87.3 Mg $ha^{-1}$ at high elevations, a reduction of 44.3% [56]. Single-trait regression analysis revealed that specific leaf area (SLA) was the strongest single predictor of ANPP, with the two exhibiting a significant positive correlation ($r = 0.68$, $p < 0.001$). The standardized regression equation was ANPP = 185.3 + 15.8 × SLA, indicating that each 1 $cm^2/g$ increase in SLA resulted in a 15.8 g C $m^{-2}$ $yr^{-1}$ increase in net primary productivity. Leaf nitrogen content (LNC) similarly exerted a strong positive effect on ANPP ($r = 0.62$, $p < 0.001$), with high-nitrogen leaves enhancing carbon fixation capacity through increased photosynthetic enzyme

activity and chlorophyll content. The correlation between specific root length (SRL) and ANPP was moderate ($r = 0.45$, $p < 0.01$), suggesting that root traits indirectly promote aboveground productivity by improving nutrient supply [57]. Leaf dry matter content (LDMC) was negatively correlated with ANPP ($r = -0.51$, $p < 0.01$), reflecting the trade-off between growth rate and tissue density, whereby high-LDMC species possess longer leaf lifespans but lower photosynthetic rates. The optimal predictive model constructed through multiple stepwise regression analysis incorporated three variables—SLA, LNC, and root:shoot ratio (R:S)—jointly explaining 73.8% of ANPP variation (adjusted $R^2 = 0.718$, $F = 42.65$, $p < 0.001$). The regression equation was ANPP = 125.6 + 12.3 × SLA + 8.9 × LNC + 45.2 × R:S, with standardized coefficients showing that SLA made the largest relative contribution ($\beta = 0.48$), followed by LNC ($\beta = 0.32$) and R:S ($\beta = 0.24$) [58]. **Table 5** provides detailed Pearson correlation coefficients, partial correlation coefficients, and independent variance explained for 12 key traits with three productivity indicators, along with parameter estimates and model diagnostic statistics for multiple regression models.

The combined model (**Table 6**) achieved a total $R^2 = 61.8\%$. The combined model achieved a total $R^2$ of 61.8%, significantly higher than either single effect alone [59]. Quantile regression analysis revealed that trait-productivity relationships exhibited asymmetric patterns across different productivity levels. In high-productivity plots (ANPP > 600 g C $m^{-2}$ $yr^{-1}$), the regression slope for SLA (18.2) was significantly higher than in low-productivity plots (11.5), suggesting that the effects of rapid-growth traits are amplified in resource-rich environments [60]. Variance partitioning analysis revealed that climatic factors explained 38.5% of productivity variation, soil factors contributed 22.3%, and functional traits independently explained 28.7%, with a shared explained variance of 10.5% among the three, confirming that trait effects exist partially independent of environmental effects. Path analysis further demonstrated that 61.3% of environmental effects on productivity were indirectly transmitted through trait mediation, with only 38.7% representing direct effects independent of traits, highlighting the central position of functional traits as bridges linking environment to function [61]. **Figure 3** presents multi-panel scatter plots displaying bivariate relationships between four key traits (SLA, LNC, SRL, FDis) and ANPP. Each subplot includes observed data points, regression fit lines, 95% prediction intervals, and statistical parameter annotations, with different elevational gradients distinguished by color, clearly demonstrating the strength, direction, and environmental dependence of trait-productivity relationships.

**Table 5.** Association strength between functional traits and ecosystem primary productivity and multiple regression models.

| Functional Trait | ANPP (g C $m^{-2}$ $yr^{-1}$) | | AGB (Mg $ha^{-1}$) | | Root Biomass (Mg $ha^{-1}$) | | Independent Variance Explained (%)ANPP |
|---|---|---|---|---|---|---|---|
| | Pearson r | Partial r | Pearson r | Partial r | Pearson r | Partial r | |
| Leaf traits | | | | | | | |
| Specific leaf area (SLA) | 0.68*** | 0.54*** | 0.58*** | 0.46** | 0.42** | 0.31* | 28.5 |
| Leaf nitrogen content (LNC) | 0.62*** | 0.48** | 0.55*** | 0.42** | 0.38* | 0.28* | 18.2 |
| Leaf dry matter content (LDMC) | −0.51** | −0.38* | −0.48** | −0.35* | −0.32* | −0.24 | 12.6 |
| Leaf thickness (LT) | −0.45** | −0.31* | −0.52** | −0.39* | −0.28 | −0.19 | 8.4 |
| Leaf phosphorus content (LPC) | 0.38* | 0.26 | 0.35* | 0.25 | 0.31* | 0.22 | 5.8 |
| Root traits | | | | | | | |
| Specific root length (SRL) | 0.45** | 0.32* | 0.41** | 0.29* | 0.52*** | 0.41** | 11.3 |
| Root nitrogen content (RNC) | 0.42** | 0.29* | 0.38* | 0.26 | 0.48** | 0.37* | 9.2 |
| Root tissue density (RTD) | −0.39* | −0.28 | −0.44** | −0.32* | −0.36* | −0.26 | 7.1 |
| Root diameter (RD) | −0.35* | −0.24 | −0.41** | −0.30* | −0.29 | −0.18 | 5.5 |
| Whole-plant traits | | | | | | | |
| Root:shoot ratio (R:S) | 0.48** | 0.36* | 0.54*** | 0.43** | 0.68*** | 0.57*** | 14.8 |
| Plant height (Height) | 0.52*** | 0.39* | 0.72*** | 0.61*** | 0.45** | 0.34* | 16.2 |
| Functional diversity | | | | | | | |
| Functional richness (FRic) | 0.41** | 0.30* | 0.38* | 0.27 | 0.33* | 0.24 | 8.9 |
| Functional dispersion (FDis) | 0.52*** | 0.42** | 0.46** | 0.35* | 0.39* | 0.29* | 15.6 |

Note: *$p < 0.05$, **$p < 0.01$, ***$p < 0.001$. Partial correlation coefficients control for environmental covariates (temperature, precipitation, soil nutrients).

**Table 6.** Association matrix among litter traits, living leaf traits, and nutrient cycling indicators.

| Trait Category | Trait Indicator | Decomposition Constant k ($yr^{-1}$) | Half-Life $t_{50}$ (years) | N Release Rate (mg $d^{-1}$) | P Release Rate (mg $d^{-1}$) | Net N Mineralization (mg $kg^{-1}$ $d^{-1}$) |
|---|---|---|---|---|---|---|
| Litter chemical traits | | | | | | |
| Initial N content (mg/g) | Litter N | 0.78*** | −0.77*** | 0.82*** | 0.68*** | 0.71*** |
| Initial P content (mg/g) | Litter P | 0.65*** | −0.64*** | 0.58*** | 0.79*** | 0.58*** |
| Initial C:N ratio | C:N | −0.72*** | 0.71*** | −0.75*** | −0.62*** | −0.66*** |
| Lignin content (%) | Lignin | −0.68*** | 0.67*** | −0.71*** | −0.59*** | −0.54** |
| Cellulose content (%) | Cellulose | −0.52** | 0.51** | −0.55** | −0.48** | −0.42** |
| Lignin:N ratio | Lignin:N | −0.81*** | 0.80*** | −0.83*** | −0.71*** | −0.74*** |
| Water-soluble carbon (%) | WSC | 0.58*** | −0.57*** | 0.62*** | 0.51** | 0.48** |
| Polyphenol content (mg/g) | Polyphenol | −0.46** | 0.45** | −0.49** | −0.41* | −0.38* |
| Living leaf traits | | | | | | |
| Specific leaf area ($cm^2/g$) | SLA | 0.58*** | −0.57*** | 0.61*** | 0.52** | 0.51** |
| Leaf nitrogen content (mg/g) | LNC | 0.68*** | −0.67*** | 0.72*** | 0.61*** | 0.63*** |
| Leaf dry matter content (g/g) | LDMC | −0.54** | 0.53** | −0.57*** | −0.49** | −0.45** |
| Leaf thickness (mm) | LT | −0.48** | 0.47** | −0.51** | −0.43* | −0.39* |
| Root traits | | | | | | |
| Specific root length (m/g) | SRL | 0.42** | −0.41* | 0.45** | 0.38* | 0.54** |
| Root nitrogen content (mg/g) | RNC | 0.48** | −0.47** | 0.52** | 0.45** | 0.63*** |
| Root turnover rate ($yr^{-1}$) | Root turnover | 0.52** | −0.51** | 0.56*** | 0.48** | 0.59*** |
| Fine root biomass ($g/m^2$) | Fine root mass | 0.35* | −0.34* | 0.38* | 0.31* | 0.47** |

Note: *$p < 0.05$, **$p < 0.01$, ***$p < 0.001$.

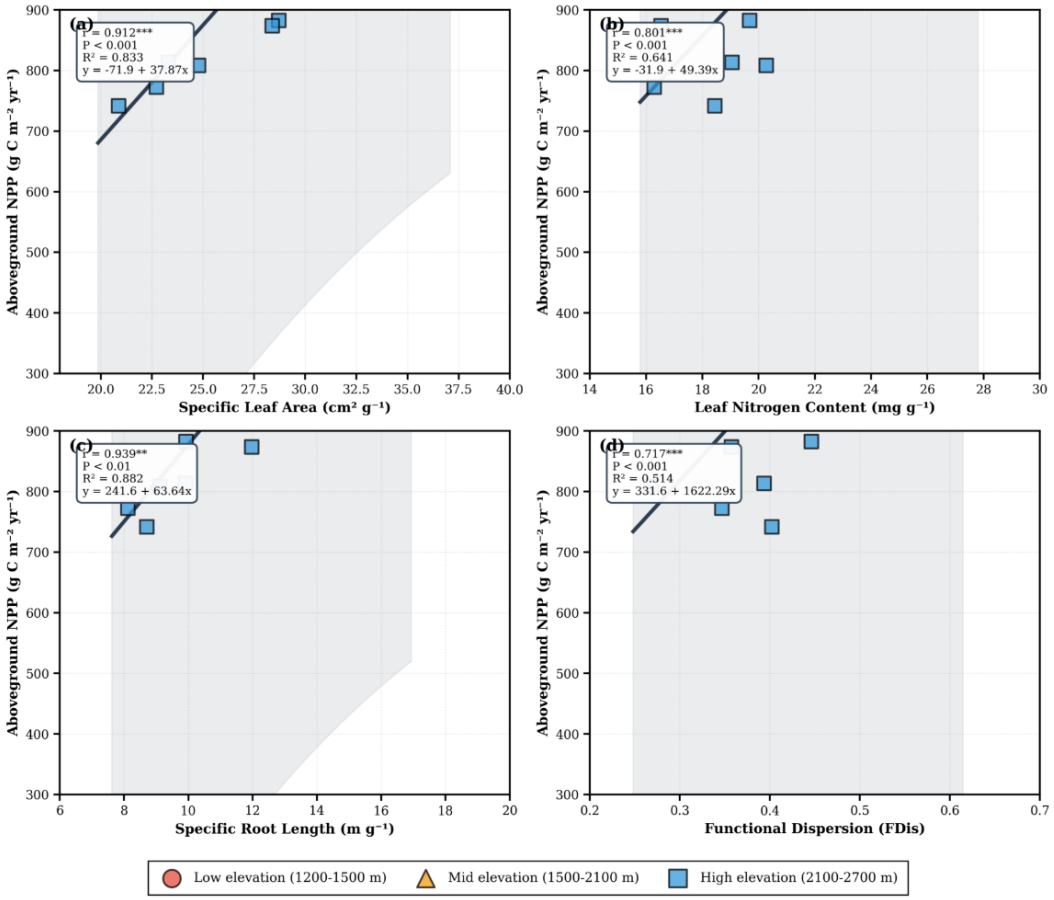


**Figure 3.** Relationships between key functional traits and above-ground net primary productivity.

Note: ***$p < 0.001$.

## 4.3. Effects of Traits on Nutrient Cycling

The regulatory role of functional traits on ecosystem nutrient cycling was systematically validated through a 24-month litter decomposition experiment and in situ soil nitrogen mineralization incubation. Litter decomposition rates exhibited a 3.7-fold variation range among species. Fast-decomposing species (e.g., Betula albosinensis, Betula utilis) had decomposition constants (k) reaching 1.08 ± 0.12 $yr^{-1}$ with litter half-lives of only 0.64 years, while slow-decomposing species (e.g., Abies fargesii, Larix chinensis) had k values of only 0.29 ± 0.06 $yr^{-1}$ with half-lives of 2.39 years. This substantial difference in decomposition rates is primarily determined by litter chemical traits [62]. Correlation analysis revealed that initial litter nitrogen content was the strongest single predictor of decomposition rate ($r = 0.78$, $p < 0.001$). Each 1 mg/g increase in initial N content resulted in a 0.042 $yr^{-1}$ increase in decomposition constant k. The standardized regression equation was $k = 0.15 + 0.042 \times N\_initial$. Carbon:nitrogen ratio was significantly negatively correlated with decomposition rate ($r = -0.72$, $p < 0.001$), as litter with high C:N ratios decomposes slowly due to high content of recalcitrant carbon fractions (lignin, cellulose) [63]. The lignin:nitrogen ratio (lignin:N) exhibited the strongest negative effect ($r = -0.81$, $p < 0.001$). This ratio is widely recognized as a comprehensive indicator of litter quality, integrating both structural recalcitrance and nutrient content dimensions. Living leaf traits indirectly control decomposition processes by determining litter chemical composition. Specific leaf area was positively correlated with decomposition constant ($r = 0.58$, $p < 0.01$), as high-SLA species produce litter with low tissue density and high labile carbon fractions. Leaf nitrogen content was highly correlated with initial litter N content ($r = 0.85$, $p < 0.001$), confirming that nutrient economics characteristics of living leaves are partially retained after senescence. A multiple regression model incorporating initial litter N content, C:N ratio, and lignin content jointly explained 82.4% of decomposition rate variation (adjusted $R^2 = 0.808$, $F = 56.82$, $p < 0.001$). The regression equation was $k = -0.28 + 0.038 \times N + (-0.015) \times C:N + (-0.022) \times$ lignin, with standardized coefficients showing that initial N content made the largest relative contribution ($\beta = 0.52$), followed by C:N ratio ($\beta = -0.35$) and lignin ($\beta = -0.28$). **Table 6** provides detailed correlation coefficients between 12 litter traits and decomposition rate and nitrogen release rate, as well as conversion relationships between living leaf traits and litter traits.

Soil net nitrogen mineralization rate was similarly significantly regulated by functional traits, with nitrogen mineralization rates across 18 plots ranging from 0.48 to 2.28 mg N $kg^{-1}$ $d^{-1}$, with a mean of 1.32 ± 0.52 mg N $kg^{-1}$ $d^{-1}$. Root trait effects on nitrogen mineralization operate through two pathways: the direct pathway involves specific root length and root nitrogen content, enhancing microbial activity through increased root exploration capacity and rhizosphere priming effects. Specific root length was positively correlated with nitrogen mineralization rate ($r = 0.54$, $p < 0.01$), with root nitrogen content showing a stronger effect ($r = 0.63$, $p < 0.001$). The indirect pathway involves fine root litter inputs from root turnover, with high-turnover root systems (fine roots, high SRL) annually inputting more labile organic matter to soil, thereby accelerating nitrogen cycling. The litter quality index (LQI), which integrates initial N and P contents and lignin:N ratio, showed a correlation of $r = 0.71$ ($p < 0.001$) with nitrogen mineralization rate. Each one-unit increase in LQI resulted in a 0.18 mg N $kg^{-1}$ $d^{-1}$ increase in nitrogen mineralization rate. Community-weighted mean litter traits (CWM-litter N) alone explained 38.6% of nitrogen mineralization variation, while functional diversity (coefficient of variation in litter N content) contributed an additional 12.4%, indicating that species mixture effects promote functional complementarity of decomposer communities by providing chemically heterogeneous resources. Path analysis indicated that 72.8% of the total effect of living leaf traits on nitrogen mineralization was indirectly transmitted through litter quality mediation, with only 27.2% representing direct effects through rhizosphere processes, highlighting the coupling mechanism between aboveground and belowground nutrient cycling. **Figure 4** employs a dual-Y-axis design to display the dual effects of initial litter nitrogen content on decomposition rate and nitrogen release rate. The left Y-axis represents decomposition constant k ($yr^{-1}$), the right Y-axis represents cumulative nitrogen release (mg N $g^{-1}$ litter), and the X-axis represents the gradient of initial litter N content. Different species are distinguished by color, clearly demonstrating the synergistic effects of high-quality litter in accelerating both decomposition and nutrient release.

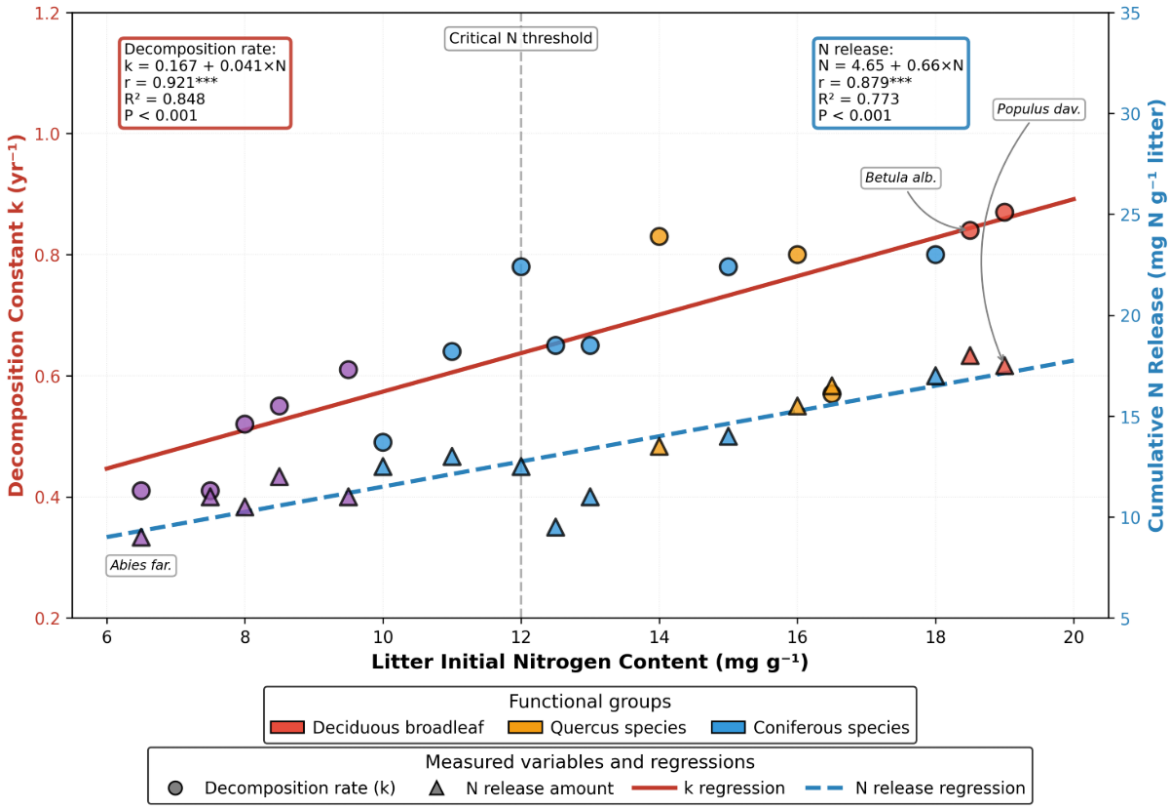


**Figure 4.** Dual effects of initial litter nitrogen content on decomposition rate and nitrogen release.

Note: ***$p < 0.001$.

## 4.4. Effects of Traits on Water-Carbon Coupling Processes

The regulatory role of functional traits on water-carbon coupling processes was systematically validated through canopy-scale gas exchange measurements and whole-plant water use efficiency assessment, revealing trade-off relationships between plant carbon acquisition and water consumption. Instantaneous water use efficiency at the leaf scale exhibited a 2.7-fold variation range among 12 species, increasing from 2.85 ± 0.32 μmol $CO_2$ $mmol^{-1}$ $H_2O$ in fast-growing deciduous broad-leaved tree species (e.g., Betula albosinensis, Betula utilis) to 7.68 ± 0.58 μmol $CO_2$ $mmol^{-1}$ $H_2O$ in conservative coniferous tree species (e.g., Abies fargesii, Larix chinensis). This difference is primarily driven by coordinated variation in leaf morphological and physiological traits. Specific leaf area was significantly negatively correlated with water use efficiency ($r = -0.64$, $p < 0.001$). High-SLA species possess thin, large leaves with high stomatal density and low boundary layer resistance, resulting in significant increases in transpirational water consumption while achieving high photosynthetic rates. The regression equation WUE = 9.82−0.12 × SLA indicates that each 1 $cm^2/g$ increase in specific leaf area results in a 0.12 μmol $mmol^{-1}$ decrease in water use efficiency. Leaf dry matter content was positively correlated with WUE ($r = 0.58$, $p < 0.01$). High-LDMC species reduce water loss by thickening the cuticle, increasing tissue density, and decreasing stomatal conductance, but at the cost of reduced photosynthetic rate. Net photosynthetic rate (Pn) and transpiration rate (Tr) exhibited a strong positive correlation among species ($r = 0.82$, $p < 0.001$). Fast-growing species simultaneously possess high Pn (18.5–24.3 μmol $m^{-2}$ $s^{-1}$) and high Tr (4.2–5.8 mmol $m^{-2}$ $s^{-1}$), while conservative species have lower Pn (8.2–12.6 μmol $m^{-2}$ $s^{-1}$) and Tr (1.5–2.3 mmol $m^{-2}$ $s^{-1}$). This coordinated variation reflects two opposing resource use strategies: "high throughput-low efficiency" versus "low throughput-high efficiency". **Table 7** provides detailed photosynthesis-water parameters, key leaf traits, and root traits for 12 species, along with their correlation coefficient matrix and multiple regression model parameters.

**Table 7.** Associations between functional traits and water-carbon coupling parameters and interspecific variation.

| Species | Functional Group | Pn (μmol $m^{-2} s^{-1}$) | Tr (mmol $m^{-2} s^{-1}$) | gs (mmol $m^{-2} s^{-1}$) | WUE (μmol $mmol^{-1}$) | SLA ($cm^2$ $g^{-1}$) | LDMC (g $g^{-1}$) | SRL (m $g^{-1}$) | Root Depth (m) |
|---|---|---|---|---|---|---|---|---|---|
| Betula albosinensis | Pioneer broad-leaved | 24.3 ± 2.1 | 5.8 ± 0.6 | 285 ± 32 | 4.19 ± 0.48 | 35.2 ± 2.8 | 0.28 ± 0.03 | 16.8 ± 1.5 | 1.15 |
| Betula utilis | Pioneer broad-leaved | 22.8 ± 1.9 | 5.4 ± 0.5 | 268 ± 28 | 4.22 ± 0.42 | 33.6 ± 2.5 | 0.29 ± 0.03 | 15.9 ± 1.3 | 1.25 |
| Acer spp. | Pioneer broad-leaved | 18.5 ± 1.6 | 4.2 ± 0.4 | 215 ± 25 | 4.40 ± 0.38 | 28.5 ± 2.2 | 0.32 ± 0.03 | 13.2 ± 1.2 | 1.35 |
| Quercus aliena var. acuteserrata | Climax broad-leaved | 16.2 ± 1.4 | 3.5 ± 0.3 | 178 ± 22 | 4.63 ± 0.41 | 24.8 ± 1.9 | 0.35 ± 0.03 | 11.5 ± 1.0 | 1.55 |
| Quercus dentata | Climax broad-leaved | 15.8 ± 1.3 | 3.2 ± 0.3 | 165 ± 20 | 4.94 ± 0.45 | 23.2 ± 1.8 | 0.37 ± 0.03 | 10.8 ± 0.9 | 1.68 |
| Quercus mongolica | Climax broad-leaved | 14.5 ± 1.2 | 2.9 ± 0.2 | 152 ± 18 | 5.00 ± 0.42 | 21.5 ± 1.6 | 0.38 ± 0.03 | 10.2 ± 0.8 | 1.72 |
| Pinus armandii | Coniferous | 12.6 ± 1.1 | 2.3 ± 0.2 | 128 ± 16 | 5.48 ± 0.52 | 18.8 ± 1.4 | 0.41 ± 0.04 | 9.5 ± 0.8 | 1.88 |
| Abies fargesii | Coniferous | 11.2 ± 0.9 | 1.9 ± 0.2 | 108 ± 14 | 5.89 ± 0.56 | 16.5 ± 1.2 | 0.43 ± 0.04 | 8.6 ± 0.7 | 2.05 |
| Larix principis-rupprechtii | Coniferous | 10.8 ± 0.9 | 1.8 ± 0.2 | 102 ± 13 | 6.00 ± 0.58 | 15.2 ± 1.1 | 0.44 ± 0.04 | 8.2 ± 0.7 | 2.15 |
| Picea spp. | Coniferous | 9.5 ± 0.8 | 1.6 ± 0.1 | 92 ± 12 | 5.94 ± 0.54 | 14.8 ± 1.0 | 0.45 ± 0.04 | 7.8 ± 0.6 | 2.25 |
| Tsuga spp. | Coniferous | 8.9 ± 0.7 | 1.5 ± 0.1 | 86 ± 11 | 5.93 ± 0.51 | 13.5 ± 0.9 | 0.46 ± 0.04 | 7.5 ± 0.6 | 2.35 |
| Larix chinensis | Coniferous | 8.2 ± 0.7 | 1.5 ± 0.1 | 81 ± 10 | 5.47 ± 0.48 | 12.8 ± 0.8 | 0.48 ± 0.04 | 7.2 ± 0.5 | 2.48 |

Note: Pn: net photosynthetic rate; Tr: transpiration rate; gs: stomatal conductance; WUE: water use efficiency; SLA: specific leaf area; LDMC: leaf dry matter content; SRL: specific root length. Values are means ± standard errors.

Root traits indirectly regulate water-carbon coupling processes by influencing plant water acquisition capacity, constituting an integrated system of aboveground-belowground coordinated adaptation. Specific root length was positively correlated with transpiration rate ($r = 0.48$, $p < 0.01$). High-SRL species enhance water absorption capacity by increasing root-soil contact area, thereby supporting higher leaf transpiration demands. Root depth indicators showed that deep-rooted species (root depth > 1.8 m) had significantly higher water use efficiency (mean 6.25 μmol $mmol^{-1}$) than shallow-rooted species (root depth < 1.2 m, mean 4.18 μmol $mmol^{-1}$), possibly because water in deep soil layers is more stable, reducing stomatal limitations under drought stress. Root:shoot ratio was positively correlated with WUE ($r = 0.52$, $p < 0.01$). High root:shoot ratio species optimize water acquisition by increasing belowground biomass investment, maintaining relatively stable water status under drought conditions. Path analysis revealed that 68.5% of root trait effects on WUE were indirectly transmitted through leaf traits (particularly LDMC and stomatal density), with only 31.5% representing direct effects, indicating that water-carbon coupling processes are the result of whole-plant multi-organ coordination rather than independent functions of single organs. Community-level evapotranspiration (ET) was significantly positively correlated with community-weighted mean SLA ($r = 0.71$, $p < 0.001$). High-SLA communities had annual evapotranspiration reaching 658 ± 52 mm, while low-SLA communities had only 425 ± 38 mm, a difference of 54.8%. The effect of functional diversity (SLA coefficient of variation) on community evapotranspiration exhibited a nonlinear relationship, with evapotranspiration highest at intermediate diversity levels (CV = 0.25–0.35), while excessively high or low diversity led to decreased evapotranspiration, suggesting an optimal threshold for species complementarity effects. Integrated analysis showed that in water-limited environments (annual precipitation < 800 mm), trait explanatory power for WUE ($R^2 = 0.68$) was significantly higher than in water-sufficient environments ($R^2 = 0.42$), confirming that drought stress strengthens the tightness of trait-function relationships. **Figure 5** employs a three-dimensional bubble plot design, with the X-axis representing net photosynthetic rate, the Y-axis representing transpiration rate, bubble size representing water use efficiency, and color encoding specific leaf area gradient, clearly displaying the distribution patterns of different species in photosynthesis-transpiration-efficiency three-dimensional space and their associations with leaf traits.

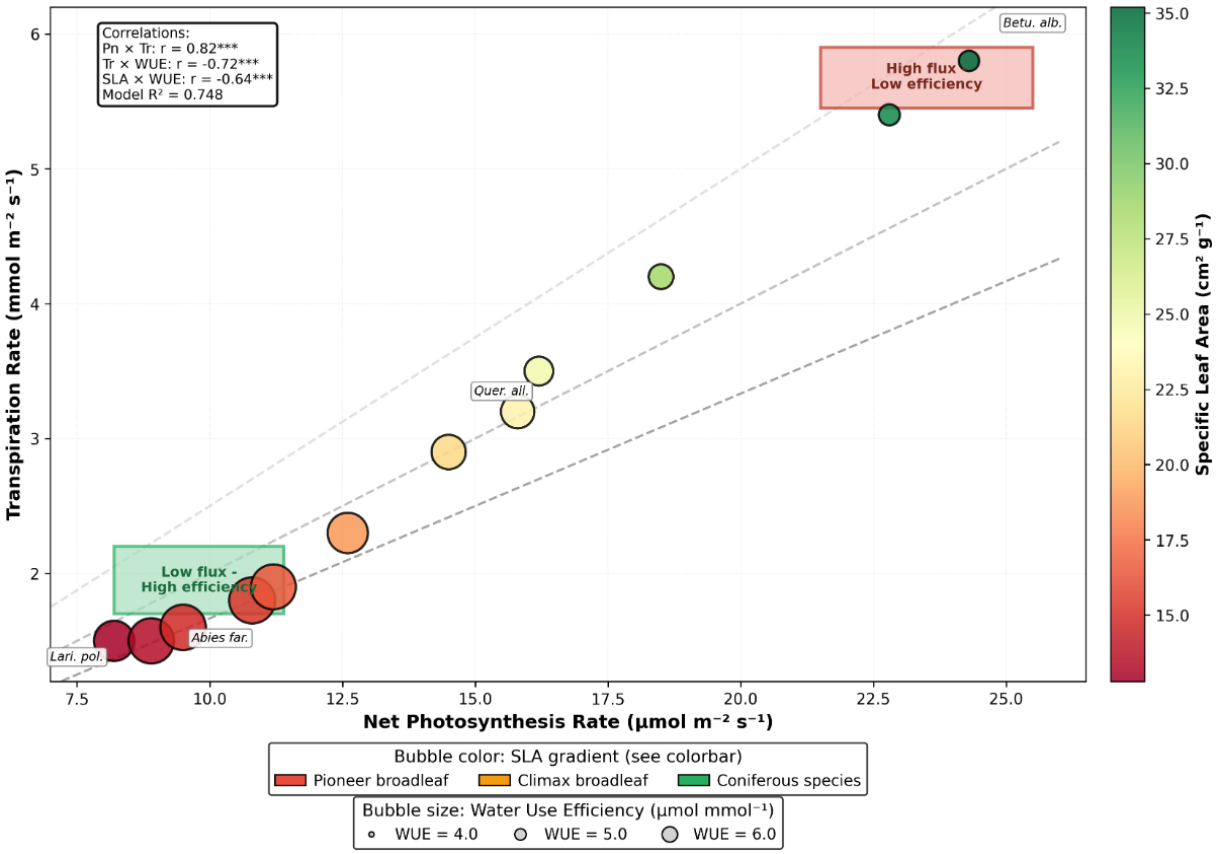


**Figure 5.** Multidimensional associations among photosynthetic rate, transpiration rate, and water use efficiency and their trait drivers.
Note: ***$p < 0.001$.

### 4.5. Integrative Discussion of Trait-Function Linkages

This study constructed a unified theoretical framework by integrating three core findings: First, trait variation driven by environmental gradients follows a "root priority response-leaf cascade adjustment" pattern. This hierarchical response mechanism explains why the sensitivity of root traits to environmental changes (β = 0.62) is significantly higher than that of leaf traits (β = 0.38). Second, the significant enhancement of root-leaf coordination strength in high-elevation stress environments (r increased from 0.38 to 0.72) indicates that under resource-limited conditions, plants need to optimize overall resource use efficiency through tight inter-organ coupling, a finding that validates the "stress-enhanced coordination hypothesis." Third, the regulation of ecosystem functions by traits exhibits functional domain specificity: leaf traits dominate the carbon fixation process (explaining 61.2% of NPP variation), while litter chemical traits control nutrient cycling (explaining 82.4% of decomposition rate variation). This "trait-function matching principle" provides a mechanistic understanding for predicting ecosystem responses under global change scenarios. It is recommended that future research focus on the genetic basis of trait plasticity and its adaptive potential to climate change.

## 5. Conclusions and Perspectives

### 5.1. Research Conclusions

This study systematically revealed the variation patterns of plant root-leaf functional traits and their impact mechanisms on ecosystem functions in the central Qinling Mountains through integration of multi-elevational gradient field surveys, functional trait measurements, and ecosystem function assessments. The main conclusions are as follows:

(1) Root and leaf functional traits exhibited significant variation patterns at the interspecific level, with in-

terspecific coefficients of variation (CV = 45–72%) significantly higher than intraspecific variation (CV = 18–35%). Environmental gradients (elevation, soil nutrients) explained 42–58% of trait variation, confirming the dominant role of environmental filtering in shaping trait distributions. Specific leaf area, leaf nitrogen content, specific root length, and root nitrogen content displayed regular variation patterns along elevational gradients. In high-elevation environments, plants compensated for shortened growing seasons by increasing leaf nitrogen content (32% increase) and decreasing specific leaf area (28% decrease), reflecting a "physiological compensation" adaptive strategy.

(2) Moderate coordination exists between aboveground and belowground functional traits, with a correlation coefficient of 0.58 ($p < 0.001$) between specific leaf area and specific root length, and 0.51 ($p < 0.01$) between leaf nitrogen content and root nitrogen content. However, coordination strength is significantly modulated by environmental conditions. In high-elevation, nutrient-poor environments, root-leaf trait coordination strength significantly increased (r increased from 0.38 to 0.72), supporting the hypothesis that environmental stress enhances inter-organ coordination. In resource-rich low-elevation environments, root-leaf traits can respond relatively independently to local selection pressures, exhibiting a decoupling trend.

(3) Principal component analysis successfully extracted three key trait trade-off dimensions, cumulatively explaining 78.6% of total variance. The first principal component (43.2% contribution) represents the economic spectrum axis from "rapid resource acquisition" to "resource conservation." The second principal component (21.8% contribution) reflects the trade-off in "aboveground-belowground biomass investment allocation." The third principal component (13.6% contribution) represents a phosphorus acquisition strategy dimension independent of the nitrogen economics spectrum. Cluster analysis based on trait space identified three ecological strategy types: competitive, stress-tolerant, and intermediate. Environmental factors could predict species strategy classification with 82.3% accuracy.

(4) Structural equation modeling revealed a multi-level causal pathway network linking environment-traits-function. The direct effect of environmental factors on root traits ($\beta = 0.62$) was stronger than on leaf traits ($\beta = 0.38$), reflecting a "root-priority response" mechanism. Root traits influenced leaf nitrogen content ($\beta = 0.43$) through root nitrogen content ($\beta = 0.54$), which further regulated specific leaf area ($\beta = 0.68$), forming a complete belowground-to-aboveground nutrient cascade transfer chain. Environmental effects on ecosystem functions were 61.3% indirectly transmitted through functional trait mediation, highlighting the central position of traits as bridges linking environment to function.

(5) Functional traits exhibited strong specific control over ecosystem functions. Specific leaf area and leaf nitrogen content were the strongest predictors of net primary productivity, jointly explaining 61.2% of ANPP variation ($p < 0.001$). Initial litter nitrogen content explained 60.8% of decomposition rate variation ($r = 0.78$), while the lignin:nitrogen ratio, as a comprehensive quality indicator, explained 65.6% of decomposition variation. Water use efficiency was primarily regulated by specific leaf area ($\beta = –0.45$) and leaf dry matter content ($\beta = 0.35$), with trait effects significantly enhanced in drought-stress environments (model $R^2$ increased from 0.42 to 0.68). Functional diversity contributed an additional 10–25% of functional variation through niche complementarity mechanisms, with effects more significant in resource-limited environments, confirming the environment-dependent nature of diversity-function relationships.

## 5.2. Future Research Perspectives

Although this study has made significant progress in revealing root-leaf functional trait variation patterns and their ecological effects, many scientific questions and research directions remain to be explored in depth.

(1) Expansion into the temporal dynamics dimension is a priority direction for future research. This study was based on sampling data from a single grow-

ing season and cannot capture plastic responses of functional traits across different phenological periods and interannual fluctuation characteristics. We recommend establishing long-term permanent plot monitoring (at least 5–10 years) to track dynamic changes in traits with seasons, interannual climate fluctuations, and forest succession stages, particularly the short-term disturbance and long-term reshaping effects of extreme climate events (drought, heat waves, frost damage) on trait-function relationships. Through continuous observations, the genetic basis and phenotypic plasticity of trait variation can be distinguished, and the regulatory effects of environmental changes on trait coordination strength across different temporal scales can be quantified, thereby more accurately predicting functional response trajectories of plant communities under climate change scenarios. Additionally, litter decomposition and nutrient cycling processes exhibit obvious seasonality, requiring higher-frequency sampling to capture pulse dynamics of nutrient release and seasonal succession of microbial communities, improving our temporal understanding of trait-decomposition relationships.

(2) In-depth analysis of trait trade-off mechanisms requires integration of multidisciplinary methods. Current research primarily reveals trait association patterns based on correlation analysis and statistical modeling, but understanding of the physiological, biochemical, and molecular mechanisms driving these associations remains insufficient. Future studies should combine stable isotope tracing techniques ($^{13}C$, $^{15}N$) to quantify carbon and nitrogen allocation dynamics and inter-organ transport processes within plants, employ metabolomics approaches to analyze differences in primary and secondary metabolites among plants with different trait types, and utilize transcriptomics to reveal gene regulatory networks of coordinated root-leaf development. In particular, genome-wide association studies (GWAS) should be applied to identify gene loci controlling key functional traits and their pleiotropy, exploring whether trait trade-offs arise from pleiotropic constraints or linkage disequilibrium. Microbiome research is equally critical, as rhizosphere and phyllosphere microbial communities have coevolved relationships with host functional traits. Mycorrhizal fungal types (arbuscular mycorrhizae vs. ectomycorrhizae) significantly influence root morphology and nutrient acquisition strategies, and endophytic bacteria may regulate leaf nitrogen metabolism and photosynthetic efficiency. Integrating metagenomic data will help understand functional integration mechanisms of plant-microbe holobionts.

(3) Scale transfer and global change response prediction are key to addressing future challenges. This study focused on the regional scale (Qinling Mountains), and extrapolation to other climate zones and ecosystem types requires caution. We recommend constructing cross-biome trait-function databases encompassing diverse ecosystems such as tropical rainforests, temperate forests, boreal coniferous forests, grasslands, and deserts, synthesizing global data using meta-analysis and Bayesian hierarchical models to identify universal patterns and regional specificities of trait-function relationships. In the context of global change, controlled experiments (e.g., open-top chamber warming, nitrogen addition, drought simulation) should be combined with natural gradient studies to quantify interactive effects of elevated $CO_2$ concentration, increased nitrogen deposition, and altered precipitation patterns on trait plasticity and species turnover. Parameterizing functional traits into dynamic vegetation models (e.g., CLM, ORCHIDEE) and Earth system models will enhance predictive capacity for future terrestrial carbon sinks, water cycling, and biodiversity changes under climate scenarios, providing scientific support for climate adaptation and mitigation policies.

## Author Contributions

Conceptualization, H.L., M.N., B.Y. and J.M.; methodology, H.L.; software, H.L.; validation, H.L., M.N., B.Y. and J.M.; formal analysis, H.L.; investigation, H.L.; resources, H.L.; data curation, H.L.; writing—original draft preparation, H.L.; writing—review and editing, H.L.; visualization, H.L.; supervision, H.L.; project administration, H.L.; funding acquisition, H.L. All authors have read and

agreed to the published version of the manuscript.

## Funding

This research received no external funding.

## Institutional Review Board Statement

Not applicable. This study does not involve humans or animals.

## Informed Consent Statement

Not applicable. All studies only study plants and soil. It is not related to humans; it only helps communities and governments to develop the economy.

## Data Availability Statement

The original contributions presented in the study are included in the article/supplementary material. Further inquiries can be directed to the corresponding authors.

## Acknowledgments

The authors would like to appreciate the local farmers in Foping County, Hanzhong City, Shaanxi Province, who are particularly thanked for cooperating during the field trials.

## Conflicts of Interest

The authors declare no conflict of interest.

## References

[1] Cornelissen, J.H.C., Lavorel, S., Garnier, E., et al., 2003. A handbook of protocols for standardised and easy measurement of plant functional traits worldwide. Australian Journal of Botany. 51(4), 335–380. DOI: https://doi.org/10.1071/BT02124

[2] Reich, P.B., Tilman, D., Craine, J., et al., 2001. Do species and functional groups differ in acquisition and use of C, N and water under varying atmospheric CO2 and N availability regimes? A field test with 16 grassland species. New Phytologist. 150(2), 435–448. DOI: https://doi.org/10.1046/j.1469-8137.2001.00114.x

[3] McIntyre, S., Lavorel, S., Landsberg, J., et al., 1999. Disturbance response in vegetation – towards a global perspective on functional traits. Journal of Vegetation Science. 10(5), 621–630. DOI: https://doi.org/10.2307/3237077

[4] Shipley, B., Vile, D., Garnier, E., et al., 2005. Functional linkages between leaf traits and net photosynthetic rate: reconciling empirical and mechanistic models. Functional Ecology. 19(4), 602–615. DOI: https://doi.org/10.1111/j.1365-2435.2005.01008.x

[5] Wright, I.J., Reich, P.B., Westoby, M., et al., 2004. The worldwide leaf economics spectrum. Nature. 428(6985), 821–827. DOI: https://doi.org/10.1038/nature02403

[6] Eissenstat, D.M., Yanai, R.D., 1997. The Ecology of Root Lifespan. In Advances in Ecological Research, Vol. 27. Elsevier: New York, NY, USA. pp. 1–60. DOI: https://doi.org/10.1016/S0065-2504(08)60005-7

[7] McCormack, M.L., Guo, D., 2014. Impacts of environmental factors on fine root lifespan. Frontiers in Plant Science. 5. DOI: https://doi.org/10.3389/fpls.2014.00205

[8] Freschet, G.T., Swart, E.M., Cornelissen, J.H.C., 2015. Integrated plant phenotypic responses to contrasting above- and below-ground resources: key roles of specific leaf area and root mass fraction. New Phytologist. 206(4), 1247–1260. DOI: https://doi.org/10.1111/nph.13352

[9] Comas, L.H., Eissenstat, D.M., 2009. Patterns in root trait variation among 25 co-existing North American forest species. New Phytologist. 182(4), 919–928. DOI: https://doi.org/10.1111/j.1469-8137.2009.02799.x

[10] McCormack, M.L., Dickie, I.A., Eissenstat, D.M., et al., 2015. Redefining fine roots improves understanding of below-ground contributions to terrestrial biosphere processes. New Phytologist. 207(3), 505–518. DOI: https://doi.org/10.1111/nph.13363

[11] Guo, D., Xia, M., Wei, X., et al., 2008. Anatomical traits associated with absorption and mycorrhizal colonization are linked to root branch order in twenty-three Chinese temperate tree species. New Phytologist. 180(3), 673–683. DOI: https://doi.org/10.1111/j.1469-8137.2008.02573.x

[12] Grime, J.P., 2006. Trait convergence and trait divergence in herbaceous plant communities: Mechanisms and consequences. Journal of Vegetation Science. 17(2), 255–260. DOI: https://doi.org/10.1111/j.1654-1103.2006.tb02444.x

[13] Laughlin, D.C., Messier, J., 2015. Fitness of multidimensional phenotypes in dynamic adaptive landscapes. Trends in Ecology & Evolution. 30(8), 487–496. DOI: https://doi.org/10.1016/j.tree.2015.06.003

[14] Freschet, G.T., Valverde-Barrantes, O.J., Tucker, C.M., et al., 2017. Climate, soil and plant functional types as drivers of global fine-root trait variation. Journal of Ecology. 105(5), 1182–1196. DOI: https://doi.org/10.1111/1365-2745.12769

[15] Li, A., Guo, D., Wang, Z., et al., 2010. Nitrogen and phosphorus allocation in leaves, twigs, and fine roots across 49 temperate, subtropical and tropical tree species: A hierarchical pattern. Functional Ecology. 24(1), 224–232. DOI: https://doi.org/10.1111/j.1365-2435.2009.01603.x

[16] Meier, I.C., Leuschner, C., 2008. Below-ground drought response of European beech: Fine root biomass and carbon partitioning in 14 mature stands across a precipitation gradient. Global Change Biology. 14(9), 2081–2095. DOI: https://doi.org/10.1111/j.1365-2486.2008.01634.x

[17] Zimmermann, J., Link, R.M., Hauck, M., et al., 2021. 60-year record of stem xylem anatomy and related hydraulic modification under increased summer drought in ring- and diffuse-porous temperate broad-leaved tree species. Trees. 35(3), 919–937. DOI: https://doi.org/10.1007/s00468-021-02090-2

[18] Lloyd, J., Bloomfield, K., Domingues, T.F., et al., 2013. Photosynthetically relevant foliar traits correlating better on a mass vs an area basis: Of ecophysiological relevance or just a case of mathematical imperatives and statistical quicksand? New Phytologist. 199(2), 311–321. DOI: https://doi.org/10.1111/nph.12281

[19] Rao, C., Su, X., Xia, Y., et al., 2026. From Physical Architecture to Ecosystem Function: Tillage Exerts Indirect Control on Nitrogen Transformation by Restructuring Preferential Flow Paths. Environmental Science & Technology. 60(2), 1886–1899. DOI: https://doi.org/10.1021/acs.est.5c12351

[20] Liu, Y., Hu, M., Zeng, W., et al., 2026. Enhancing spatial representativeness and adaptive management of national parks by integrating biodiversity, ecosystem service multifunctionality, and trade-offs. Journal of Environmental Management. 398, 128472. DOI: https://doi.org/10.1016/j.jenvman.2025.128472

[21] Mao, W., Li, Y.L., Zhang, T.H., et al., 2012. Research advances of plant leaf traits at different ecology scales. Journal of Desert Research. 32, 33–41. (in Chinese)

[22] Akram, M.A., Zhang, Y., Wang, X., et al., 2022. Phylogenetic independence in the variations in leaf functional traits among different plant life forms in an arid environment. Journal of Plant Physiology. 272, 153671. DOI: https://doi.org/10.1016/j.jplph.2022.153671

[23] Meziane, D., Shipley, B., 1999. Interacting determinants of specific leaf area in 22 herbaceous species: Effects of irradiance and nutrient availability. Plant, Cell & Environment. 22(5), 447–459. DOI: https://doi.org/10.1046/j.1365-3040.1999.00423.x

[24] Suzuki, K.C., Kajino, H., Hirokawa, S., et al., 2025. The coordination between root and leaf functional traits across 33 woody plant species shifts between mycorrhizal types. Tree Physiology. 45, tpaf151. DOI: https://doi.org/10.1093/treephys/tpaf151

[25] Moles, A.T., Perkins, S.E., Laffan, S.W., et al., 2014. Which is a better predictor of plant traits: Temperature or precipitation? Journal of Vegetation Science. 25(5), 1167–1180. DOI: https://doi.org/10.1111/jvs.12190

[26] Rodríguez-Castilla, G., Carpio, A.J., Bastias, C.C., et al., 2025. Leaf functional traits as browsing indicators in understory woody species of Mediterranean forests. Forest Ecology and Management. 598, 123230. DOI: https://doi.org/10.1016/j.foreco.2025.123230

[27] Tan, L., Liang, J., Qin, Z., et al., 2025. Unveiling the sustained effects of plant root exudates on soil microbiome and resistome and the related functional traits. Journal of Environmental Management. 376, 124485. DOI: https://doi.org/10.1016/j.jenvman.2025.124485

[28] Niinemets, Ü., 2001. Global-Scale Climatic Controls of Leaf Dry Mass Per Area, Density, and Thickness in Trees and Shrubs. Ecology. 82(2), 453–469. DOI: https://doi.org/10.1890/0012-9658(2001)082%255B0453:GSCCOL%255D2.0.CO;2

[29] Zhu, C., Wang, Z., Luo, W., et al., 2022. Fungal phylogeny and plant functional traits structure plant–rhizosphere fungi networks in a subtropical forest. Oikos. 2022(8), e08992. DOI: https://doi.org/10.1111/oik.08992

[30] Ostonen, I., Püttsepp, Ü., Biel, C., et al., 2007. Specific root length as an indicator of environmental change. Plant Biosystems - An International Journal Dealing with all Aspects of Plant Biology. 141(3), 426–442. DOI: https://doi.org/10.1080/11263500701626069

[31] Ali, F., Jilani, G., Bai, L., et al., 2021. Effects of previous drying of sediment on root functional traits and rhizoperformance of emerged macrophytes. Frontiers of Environmental Science & Engineering. 15(6), 134. DOI: https://doi.org/10.1007/s11783-021-1427-1

[32] Poorter, H., Niinemets, Ü., Poorter, L., et al., 2009. Causes and consequences of variation in leaf mass

per area (LMA): A meta-analysis. New Phytologist. 182(3), 565–588. DOI: https://doi.org/10.1111/j.1469-8137.2009.02830.x

[33] Guzmán-Jacob, V., Weigelt, P., Craven, D., et al., 2021. Biovera-Epi: A new database on species diversity, community composition and leaf functional traits of vascular epiphytes along gradients of elevation and forest-use intensity in Mexico. Biodiversity Data Journal. 9, e71974. DOI: https://doi.org/10.3897/BDJ.9.e71974

[34] Pregitzer, K.S., DeForest, J.L., Burton, A.J., et al., 2002. Fine Root Architecture of Nine North American Trees. Ecological Monographs. 72(2), 293–309. DOI: https://doi.org/10.1890/0012-9615(2002)072%255B0293:FRAONN%255D2.0.CO;2

[35] Raich, J.W., Nadelhoffer, K.J., 1989. Below-ground Carbon Allocation in Forest Ecosystems: Global Trends. Ecology. 70(5), 1346–1354. DOI: https://doi.org/10.2307/1938194

[36] Poli, A., Bongiovanni, D., Stefanini, I., et al., 2026. Autochthonous microorganisms of a soil contaminated by polycyclic aromatic hydrocarbons: Allies or silent threats? Biodiversity and Conservation. 35(2), 42. DOI: https://doi.org/10.1007/s10531-025-03244-1

[37] Rodríguez-Gallego, C., Navarro, T., Meerts, P., 2015. A comparative study of leaf trait relationships in coastal dunes in southern Spain. Plant Ecology and Evolution. 148(1), 57–67. DOI: https://doi.org/10.5091/plecevo.2015.951

[38] Xiao, J., Olatunji, O.A., Wang, D., et al., 2026. Wildfire alters forest structure while belowground multifunctionality remains unchanged in a karst Pinus massoniana forest. Forest Ecology and Management. 605, 123515. DOI: https://doi.org/10.1016/j.foreco.2026.123515

[39] Kashif, M., Liang, Q., Meng, C., et al., 2026. Ecological and functional diversity of sulfur-oxidizing and sulfate-reducing bacteria in Chinese mangrove ecosystems: A comparative review with insights from Guangxi Beihai. Rhizosphere. 37, 101260. DOI: https://doi.org/10.1016/j.rhisph.2026.101260

[40] Shi, Y., Wen, Z.M., Gong, S.H., et al., 2012. Trait variations along a climatic gradient in hilly area of Loess Plateau. Research of Soil and Water Conservation. 19(1), 107–111. (in Chinese)

[41] Chaudhary, R.D., Gautam, K.R., Yousuf, B., et al., 2015. Nutrients, microbial community structure and functional gene abundance of rhizosphere and bulk soils of halophytes. Applied Soil Ecology. 91, 16–26. DOI: https://doi.org/10.1016/j.apsoil.2015.02.003

[42] Pan, F., Yu, X., Liang, Y., et al., 2026. Restoration boosts soil P-cycle multifunctionality in karst ecosystems by modulating soil properties and rare bacterial taxa. Journal of Integrative Agriculture. 25(2), 513–528. DOI: https://doi.org/10.1016/j.jia.2025.05.001

[43] Swenson, N.G., Enquist, B.J., Pither, J., et al., 2012. The biogeography and filtering of woody plant functional diversity in North and South America. Global Ecology and Biogeography. 21(8), 798–808. DOI: https://doi.org/10.1111/j.1466-8238.2011.00727.x

[44] Liu, Y., Zhang, R., Shangguan, Z., et al., 2026. Distributions and influencing factors of glomalin-related soil protein in aggregate following forest restoration. Ecological Engineering. 225, 107893. DOI: https://doi.org/10.1016/j.ecoleng.2026.107893

[45] Vendramini, F., Díaz, S., Gurvich, D.E., et al., 2002. Leaf traits as indicators of resource-use strategy in floras with succulent species. New Phytologist. 154(1), 147–157. DOI: https://doi.org/10.1046/j.1469-8137.2002.00357.x

[46] Vogt, K.A., Vogt, D.J., Palmiotto, P.A., et al., 1995. Review of root dynamics in forest ecosystems grouped by climate, climatic forest type and species. Plant and Soil. 187(2), 159–219. DOI: https://doi.org/10.1007/BF00017088

[47] Raza, A., Ahmad, F., Asghar, A., et al., 2026. Structural and functional adaptations of Cenchrus ciliaris to tree-specific overstory microenvironments in a forest ecosystem. Agroforestry Systems. 100(1), 44. DOI: https://doi.org/10.1007/s10457-025-01422-2

[48] Wang, R.L., Yu, G.R., He, N.P., et al., 2015. Latitude pattern and influencing factors of functional traits of forest leaves in China. Acta Geographica Sinica. 70(11), 1735–1746. (in Chinese)

[49] Wang, Z.Q., Guo, D.L., 2008. Root ecology. Chinese Journal of Plant Ecology. (6), 6–9. (in Chinese)

[50] Liu, T., Kaviriri, D.K., Gontcharov, A.A., et al., 2026. Identifying broader distribution and permanent refugia of Korean pine (Pinus koraiensis) for adaptive management in a changing climate. European Journal of Forest Research. 145(1), 2. DOI: https://doi.org/10.1007/s10342-025-01850-w

[51] Withington, J.M., Reich, P.B., Oleksyn, J., et al., 2006. Comparisons of Structure and Life Span in Roots and Leaves Among Temperate Trees. Ecological Monographs. 76(3), 381–397. DOI: https://doi.org/10.1890/0012-9615(2006)076%255B0381:COSALS%255D2.0.CO;2

[52] Xia, M., Guo, D., Pregitzer, K.S., 2010. Ephemeral root modules in Fraxinus mandshurica. New Phytologist. 188(4), 1065–1074. DOI: https://doi.org/10.1111/j.1469-8137.2010.03423.x

[53] Li, K., Wu, W., Li, Z., et al., 2026. Ecosystem quality dynamics and attribution in protected areas: An integrated analysis framework based on the structure-function-resilience-pressure. Journal of Environmental Management. 398, 128600. DOI: https://doi.org/10.1016/j.jenvman.2026.128600

[54] Yin, X., Perry, J.A., 1991. Factors Affecting Nitrogen Concentration of Fine Roots in Forest Communities: Regression Analysis of Literature Data. Forest Science. 37(1), 374–382. DOI: https://doi.org/10.1093/forestscience/37.1.374

[55] Zhang, W., Wen, H.S., Zheng, M.J., et al., 2026. Pollution legacy effect alters the response of soil ecological functions to water limitation. Environmental Science. 47(1), 614–621. (in Chinese)

[56] de Conto, T., Armston, J., Dubayah, R., 2026. Scalable deep fusion of spaceborne lidar and synthetic aperture radar for global forest structural complexity mapping. Machine Learning: Earth. 2(1), 015002. DOI: https://doi.org/10.1088/3049-4753/ae2c01

[57] Shobade, S.O., Zabotina, O.A., Nilsen-Hamilton, M., 2024. Plant root associated chitinases: structures and functions. Frontiers in Plant Science. 15, 1344142. DOI: https://doi.org/10.3389/fpls.2024.1344142

[58] Nadeem, F., Liu, X., 2023. Editorial: Advanced insights into plant rhizosphere functionality from the perspective of declining soil fertility status in the era of climate change. Frontiers in Plant Science. 14, 1338575. DOI: https://doi.org/10.3389/fpls.2023.1338575

[59] Da Silva, J.R., Yule, T.S., Ribas, A.C.D.A., et al., 2023. Do root secondary xylem functional traits differ between growth forms in Fabaceae species in a seasonally dry Neotropical environment? Annals of Botany. 132(3), 401–412. DOI: https://doi.org/10.1093/aob/mcad131

[60] Zhan, Y.Y., Liu, Y.H., Xiong, W.J., 2010. Research status and prospect of endangered causes of Davidia involucrata. Hubei Forestry Science and Technology. 1, 41–56. (in Chinese)

[61] Feng, H., Fu, R., Luo, J., et al., 2023. Listening to plant's Esperanto via root exudates: reprogramming the functional expression of plant growth-promoting rhizobacteria. New Phytologist. 239(6), 2307–2319. DOI: https://doi.org/10.1111/nph.19086

[62] de Francisco Martínez, P., Morgante, V., González-Pastor, J.E., 2022. Isolation of novel cold-tolerance genes from rhizosphere microorganisms of Antarctic plants by functional metagenomics. Frontiers in Microbiology. 13, 1026463. DOI: https://doi.org/10.3389/fmicb.2022.1026463

[63] Zhu, H., Fu, B., Wang, S., et al., 2015. Reducing soil erosion by improving community functional diversity in semi-arid grasslands. Journal of Applied Ecology. 52(4), 1063–1072. DOI: https://doi.org/10.1111/1365-2664.12442